https://doi.org/10.59761/RCR5147

Synthesis of acrylic acid and acrylates from CO_2 and ethylene — the thorny path from dream to reality

Nikolai Yu. Kuznetsov,[a,b,c] **Anton L. Maximov,**[a,b] **Irina P. Beletskaya**[a,b]

[a] *Lomonosov Moscow State University, 119991 Moscow, Russia*
[b] *A.V.Topchiev Institute of Petrochemical Synthesis, Russian Academy of Sciences, 119991 Moscow, Russia*
[c] *A.N.Nesmeyanov Institute of Organoelement Compounds, Russian Academy of Sciences, 119991 Moscow, Russia*

The development of atom-economical and efficient processes for obtaining a variety of chemical products using CO_2 as C_1-synthon plays an increasingly important role in modern scientific and technological research. Due to the inertness of CO_2 many extremely attractive routes to valuable chemical products turn out to be impossible to implement, particularly for thermodynamic reasons, leaving one only dreaming about them as something unattainable. This review demonstrates how the catalytic coupling of ethylene and CO_2 into acrylic acid, once considered a 'dream reaction' has not only become a reality, but has also evolved into the category of technological processes. The key stages of the long-term development of this unique reaction from the discovery of metal activation of CO_2 and stoichiometric preparation of metallalactones to catalytic synthesis using a variety of metal-catalysts (Ni, Pd, Ru, Rh) showcase the ingenuity and skill of researchers as well as an example of consistent development in this field of chemistry. We believe that this remarkably successful example will inspire scientists to tackle any 'impossible' problems.
The bibliography includes 117 references.
Keywords: acrylic acid, sodium acrylate, CO_2, carbon dioxide, catalysis.

Contents

1. Introduction

Acrylic acid (AA), CH_2=$CHCO_2H$ is the first representative of α,*β*-unsaturated carboxylic acids. Anhydrous (glacial) AA is a colorless liquid with a boiling point of 141.0 °C and a melting point of 13.5 °C. In terms of acidity, AA is slightly stronger than acetic acid with a dissociation constant of 5.5×10^{-5} (pKa 4.26). It is completely miscible with water and has the lowest freezing point of –12.5 °C with 37% water content. In chemical properties, AA is similar to both carboxylic acids and unsaturated compounds, displaying a significant ability to polymerize. Due to this, the surface liquid where the polymerization inhibitor (phenothiazine, hydroquinone or its monomethyl ester) is concentrated must not be removed from the solidified AA and the solidified acid must not be heated above 30 °C.[1]

Despite its high chemical activity, AA causes little harm to the environment and living organisms. Additionally, AA is a biodegradable compound that degrades rapidly in light, soil and water. Apparently, due to this, AA is rare in nature. It is known to be produced by seaweeds and has also been found in the rumen (first stomach) fluid of sheep.[†]

N.Yu.Kuznetsov. Doctor of Chemistry, Head of the Laboratory of Small Molecule Activation at TIPS RAS, Senior Researcher at INEOS RAS. E-mail: nkuznff@ips.ac.ru
Current research interests: stereoselective organic synthesis of natural, biologically active azaheterocyclic compounds; development of new methods and reagents for allylation based on highly active allylic triorganoboranes; new catalytic methods for carboxylation using CO_2 of unsaturated hydrocarbons, including functionalized derivatives, epoxides, hydroxyaromatic compounds to create methods suitable not only for laboratory but also low-tonnage industrial synthesis.
A.L.Maximov. Doctor of Chemical Sciences, Professor, Corresponding member of RAS, Director of TIPS RAS, Professor at the Chemical Department of MSU. E-mail: max@ips.ac.ru
Current research interests: petroleum chemistry, oil refining, renewable feedstock refining, biorefining, homogeneous and heterogeneous catalysis, green chemistry, immobilized catalysts.
I.P.Beletskaya. Full member of RAS, Doctor of Sciences, Professor at the Chemical Department of MSU, Chief Researcher at TIPS RAS. E-mail: beletska@org.chem.msu.ru
Current research interests: organic synthesis, organoelement compounds, organometallic chemistry, catalysis with transition metal complexes, nanocatalysis, organocatalysis, CO_2 utilization, reaction mechanisms.

[†] https://www.inchem.org/documents/ehc/ehc/ehc191.htm (accessed 01.08.2024).

Received 10 May 2023

As a member of an important class of carboxylic acids, AA has high relative content of carbon dioxide, up to 61% of the gross weight of the AA molecule. It serves as an excellent example of efficient CO_2 utilization. Notably, among various products of organic synthesis obtained from CO_2, organic acids such as formic acid, hydroxybenzoic acids, adipic acid, etc. constitute a significant part (Fig. 1).[2–16] Additionally, CO_2 has several advantages as a reagent, including its affordability, non-flammability, non-toxicity, widespread availability and inexhaustibility as a main component of industrial gases used in chemical production, thermal and power plants, etc. and as a constituent of air (>0.04%). The tools for reactions with CO_2 is constantly expanding to include a wide range of catalytic, photocatalytic and electrochemical methods.[17] This field of chemistry is progressing rapidly, with new CO_2 carboxylation methods that do not even require special equipment and can operate at normal pressure and temperature. In addition to the obvious advantages of this C_1-synthon (see Fig. 1), there is another powerful incentive for its use in industrial synthesis.

As the primary greenhouse gas in the atmosphere, CO_2 is responsible for ongoing global climate change and the resulting negative impacts on human life.[18–20] The implementation of the 2015 Paris Climate Agreement,[‡] which aims to reduce CO_2 emissions, requires a fundamental restructuring of the technological sector. Energy-efficient, atom-efficient processes based on CO_2 recycling will be crucial in this transition. In this technological paradigm, precise control over the amount of CO_2 emitted is a key factor that defines the quality of the technology and even the products themselves.

The proposed methodology for estimating emitted CO_2 includes not only the production stages, but also the entire 'life cycle' of the product, including its processing and decomposition as waste.[6] Creating products with high CO_2 content is undoubtedly relevant and economically feasible. However, achieving this goal is challenging because many chemical transformations of CO_2 are thermodynamically prohibited. This is due to the high stability of the carbon dioxide molecule, which in the potential energy well is located much lower than other compounds ($\Delta G_R^0 = -396$ kJ mol^{-1}). Similar to the water molecule, it is the most stable product of combustion and oxidation processes.[2] Consequently, the Gibbs energy of many of its reactions turns out to be positive, primarily due to the energy costs of CO_2 activation and changes in the degree of oxidation of carbon atom.

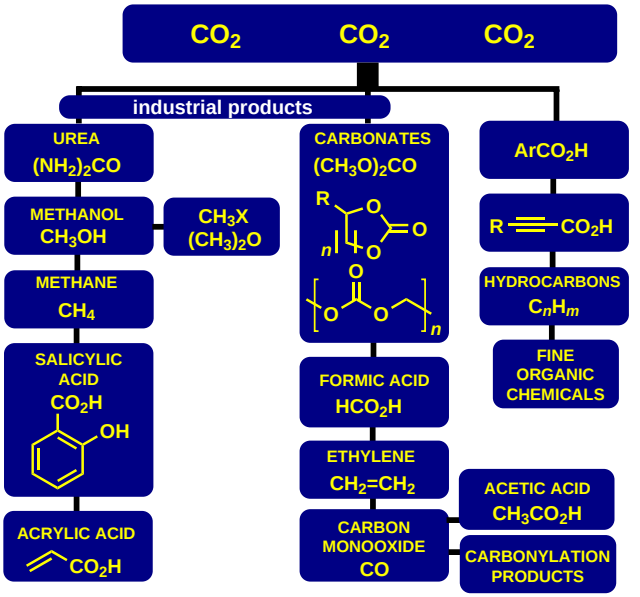

Figure 1. Valuable products derived from carbon dioxide.[8]

[‡] https://unfccc.int/sites/default/files/russian_paris_agreement.pdf (accessed 01.08.2024).

Based on CO_2 and other small molecules, one can envision several highly atom-efficient pathways for synthesizing compounds of great value to industry. However, these pathways may be thermodynamically or due to other energy factors or technologically unattainable. In this case such processes are often referred to as 'dream reactions' because they are highly desirable yet challenging to achieve. Examples of 'dream reactions' include the synthesis of methanol by direct oxidation of methane, where the problem of selectivity is of fundamental importance, because methanol oxidizes much easier than the starting methane (Scheme 1). CO_2 endothermic syntheses of formic acid ($\Delta G_R^0 = +32.9$ kJ mol^{-1}), acetic acid ($\Delta G_R^0 = +55.0$ kJ mol^{-1}), adipic acid ($\Delta G_R^0 = +77.4$ kJ mol^{-1}), dimethyl carbonate ($\Delta G_R^0 = +26.2$ kJ mol^{-1}), phenylisocyanate ($\Delta G_R^0 = +306.6$ kJ mol^{-1}), and other aryl derivatives are also considered 'dream reactions'. These reactions require a combination of special approaches, to alter the thermodynamics of the process and significantly increase their rate.

Therefore, the most important role in the implementation of such transformations is assigned to catalytic systems. Although they do not change the thermodynamics of the process, they allow for lowering the energy barrier, thus, opening the possibility of more effectively controlling the chemical equilibrium and shifting it toward the reaction products. In particular, in the catalytic synthesis of formic acid, its conversion to the solvated salt form allowed for making the process not only thermodynamically favorable but also catalytically efficient with TON values reaching several million.[21,22]

Among the 'dream reactions' (see Scheme 1), the synthesis of AA holds a special significance and a revealing history, from the initial idea to the testing of the technological scheme of synthesis in a laboratory. Several scientific groups have achieved remarkable success in implementing this challenging reaction,[23–27] although one step still separates researchers from turning the dream into reality. Given this, each of us can contribute to taking this important step by combining the achievements of many chemists to improve this breakthrough reaction and create an efficient industrial technology based on it.

Scheme 1

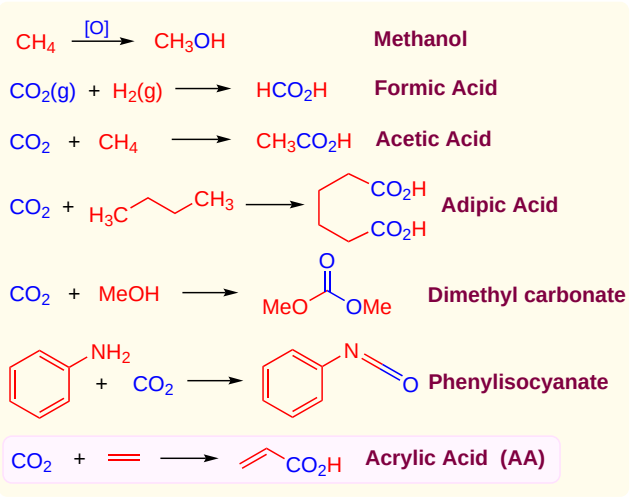

Therefore, this paper will analyze the most important stages in the development of this process and the existing obstacles that complicate the transition to an efficient industrial synthesis of AA.

AA is an important industrial product, as evidenced by its impressive global production forecasted at 7.8 million tons in 2024.[§] Derivatives of AA such as esters and salts as well as polymers based on it are widely used in various industries and households. These derivatives are utilized in coatings, paints, superabsorbents, adhesives, sealants, polymer fibers (such as Acrilan, Creslan, Dralon, Vonnel, *etc.*), components for 3D printing, reagents for oil production, water purification and more.[1] Thanks to the ease of radical poly- and copolymerization, a wide variety of acrylic polymers can be achieved by using different types of initiating systems. The choice of the type of ether radical controls the degree of polymer adhesion or fiber smoothness. Polyacrylates hardly ever yellow in direct sunlight because they absorb UV radiation below 290 nm. Copolymers of acrylate ester and methacrylate ester ('pure acrylates') have excellent UV light resistance, making them ideal binders for transparent coatings with low pigment content, which is among the important advantages of polyacrylates.[28] Acrylic fibers are also a major source for pyrolysis into carbon fiber.[29] Water-soluble polyacrylic acid and its salts with a molecular weight of 2–5 thousand are utilized as deposit inhibitors, sludge dispersants in cooling water systems, pigments or paper coating materials.[30] Copolymers with a small number of hydrophobic side groups are also useful as fracturing fluids in oil drilling.[31] Cross-linked sodium polyacrylate is a common absorbent in baby and adult diapers,[32–34] feminine hygiene products.[35] It should be noted that the market share of sodium (poly)acrylate involved in the production of superabsorbents[36] reaches 70% and is an important component of the total volume of AA produced.[¶] Cross-linked polymers of acrylic or methacrylic acid neutralized to more than 50 mol.% are also used to provide high water retention capacity and viscosity of gypsum.[37] The cross-linked water-absorbing AA polymer is integrated into the formulations of prolonged-acting tablets.[38] A mixture of water swelling particles of anionic AA polymer or methacrylic acid and their soluble salts and cationic aminoacrylate and aminoalkylacrylamide polymers are used in precoated adhesives for wallpapers.[39]

2. Industrial processes for the production of AA

Given the demand for acrylate derivatives, several industrial processes have been developed for AA production. In 1945 Walter Reppe first developed the process of stoichiometric alkoxy(hydroxy)hydrocarbonylation of acetylene using nickel carbonyl (Scheme 2).[40] A quarter mole of nickel carbonyl was added dropwise to an acetylene-saturated alcoholic or aqueous solution containing 0.5 equiv. of HCl under normal pressure to produce ethyl acrylate or AA in 80% yield. However, this method of conducting the process is not suitable for industrial synthesis due to the release of explosive hydrogen, difficulty of regeneration of $Ni(CO)_4$ and its high toxicity. Despite these limitations, it laid the foundation for a more efficient method. It was discovered that introducing CO (up to 2 bar) into the reaction could significantly reduce the toxic nickel carbonyl loading, and a method for its regeneration *via* ammoniacate was developed. This modernized process was utilized by Rohm & Haas and Toagosei to produce methyl acrylate.[41] Later, Reppe and Stadler (BASF) developed a catalytic method for the synthesis of AA. This method involved carrying out the reaction under pressure with a mixture of acetylene and CO (1 : 1) at 170–220 °C in the presence of nickel(II) and copper(II) halides.[42]

Scheme 2

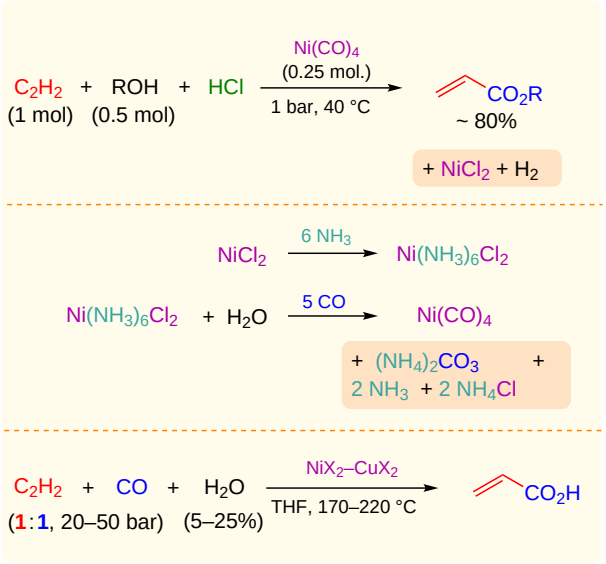

The ketene method was successfully used in the synthesis of AA and its esters (Scheme 3). Ketene is formed by cracking acetic acid or acetone and then reacts with formaldehyde to produce *β*-propiolactone. The *β*-propiolactone is subsequently subjected to alcoholysis or hydrolysis in the presence of sulfuric acid. The intermediate *β*-hydroxy-derivative is dehydrated to form AA or its ester.[41] This method, although historically significant, is not commonly employed due to the toxicity and carcinogenicity of *β*-propiolactone, as well as its multistep process. In 2016, a new selective catalytic process for producing *β*-propiolactone from ethylene oxide and CO (obtained electrochemically from CO_2) on a cobalt catalyst was developed.[††,43,44] This technology significantly enhances safety, as *β*-propiolactone can be used in the form of a harmless polymer poly(3-hydroxypropionate). This polymer can be transported to the AA production site without special precautions, straight for the conversion of the polymer to glacial AA.

In the ethylenecyanohydrin process (1941–1945), ethylene oxide is treated with hydrocyanic acid to form ethylene-cyanohydrin (Scheme 4). The ethylenecyanohydrin is then

Scheme 3

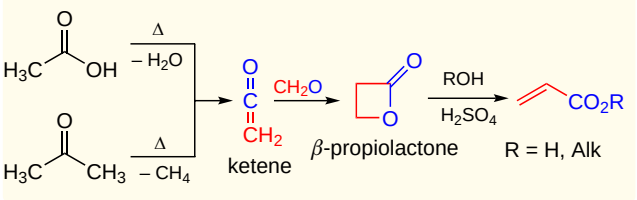

[§] https://www.mordorintelligence.com/industry-reports/acrylic-acid-market (accessed 01.08.2024).

[¶] https://www.chemanalyst.com/Pricing-data/superabsorbent-polymer-1144 (accessed 01.08.2024).

[††] https://www.novomer.com/product in Acrylic acid section (accessed 01.08.2024).

dehydrated to acrylonitrile and further hydrolyzed in the presence of sulfuric acid. This process was utilized by several industrial companies, but was discontinued due to issues related to toxic HCN and waste NH_4HSO_4.[1,45]

Scheme 4

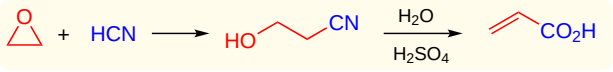

In the early 1960s, due to the decreasing price of acrylonitrile, which could be produced more safely and efficiently through the catalytic ammoxidation of propylene, Standard Oil Co. (SOHIO) and Societe Ugine Company developed their own process for the production of AA through the hydrolysis of nitrile (Scheme 5).[46] The hydrolysis process consists of two stages: first, the hydrolysis of nitrile to acrylamide at 90 °C in the presence of sulfuric acid, and then the methanolysis of the acrylamide to methyl acrylate at 150 °C. This method has been successfully utilized by several companies in Japan and China. However, despite its simplicity and efficiency, there are significant drawbacks to this process. One major issue is the generation of a large amount of ammonium hydrosulfate waste, which is difficult to process. Additionally, the process relies heavily on the cost of propylene, which is the raw material for acrylonitrile. Furthermore, up to 10% of toxic hydrocyanic acid is produced during the synthesis of acrylonitrile. Nevertheless, it is noted that Japan still continues to employ this method for the synthesis of methyl acrylate.[1]

Scheme 5

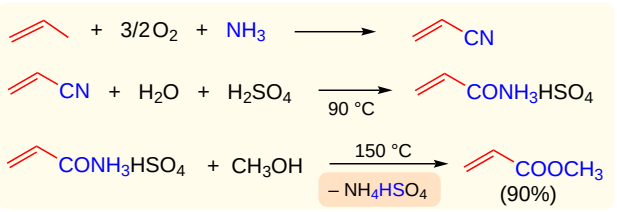

One promising trend in AA production is the use of various types of renewable raw materials such as glucose,[47] glycerol,[48] lactic acid derivatives (lactide derivatives),[49,50] furfural[51] and others. Despite their environmentally friendly nature, these methods are multi-stage and require further research to achieve economic feasibility and meet other parameters necessary for industrial production.

To date, the primary method for large-scale production of AA is the two-stage oxidation of propylene on heterogeneous catalysts to convert propylene to acrolein and then to AA, making it a highly efficient process (Scheme 6).[1,45] Each stage of this process has its own kinetics and optimal conditions (stage 1 – 320 °C, stage 2 – 220 °C) and requires the use of unique polymetallic oxide catalysts including oxides of Bi, Mo, Fe, W, Si, K, V, Cu, Cr, and Al.[45] Typical catalytic compositions are shown in Scheme 6. Despite the complex composition of the catalysts, both reaction steps have high yields (94% and 98%) and selectivity (96% for acrolein). The process uses the hazardous oxidizing agent oxygen and the relatively expensive propylene. The method involves two steps, and the catalysts have a very specific formula. Due to significant differences in the conditions under which each stage is carried out, it has not yet been possible to elaborate an industrial one-step process.

Scheme 6

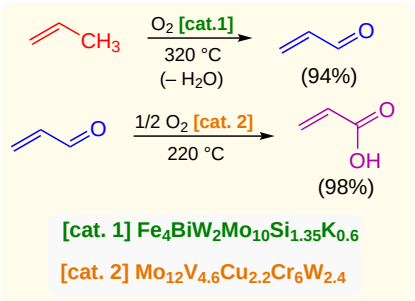

We can also mention the method of synthesizing AA through the direct oxidation of propane using mixed Mo – V – Te – Nb-oxide catalysts. This approach has been studied by several companies, including Mitsubishi Rayon, Rohm & Haas, Toagosei, Arkema, BASF, *etc*. However, as of now, industrial technology for this process has not been developed.[52–56]

The primary advantages of the 'dream reaction', which involves the production of AA from ethylene and CO_2 (see Scheme 1), are its one-stage process and the availability of reagents. CO_2 is a waste product with an emission volume of gigatonnes, and ethylene, one of the most abundant products in petrochemical synthesis, is more competitive than propylene.

Both alkenes, ethylene and propylene, are produced through thermal cracking (steam cracking) of hydrocarbons at high temperature, resulting in a mixture consisting mainly of ethylene, propylene and butylene. The composition and yield of the main products, namely ethylene and propylene, depend on the feedstock used, which includes ethane/propane/naphtha (ligroin)/gasoil (Table 1).[57]

Based on the efficiency of the respective processes, the relative cost of ethylene production from different feedstock sources is as follows: ethane/propane/naphtha (ligroin)/gasoil = 1.0/1.2/1.4/1.5. Therefore, the most cost-effective method is ethane cracking, while propylene production is significantly more expensive due to its low yield. It is important to note that these ratios do not account for the difference in the cost of the feedstock itself or the impact of volatility in the crude oil prices. As of 2024, Brent crude oil prices remain >$80 per barrel. Consequently, in the first quarter of 2024, propane prices in Asian spot markets reached as high as $660 per ton, while ethane prices were around $230 per ton and naphtha prices were as high as $667 per ton.[‡‡] In South America prices for the corresponding raw materials were $439, $143 and $671 per ton (Table 2).[§§]

Thus, the synthesis of AA through the carboxylation of ethylene offers significant advantages compared to the current method of oxidizing propylene, which is more costly to produce.

Table 1. Gas composition of alkene mixture depending on the type of hydrocarbon feedstock.[57]

Product (%)	Raw materials			
	Ethane	Propane	Naphtha	Gasoil
Ethylene	**76**	**42**	**31**	**23**
Propylene	3	16	16	14
C_4	2	5	9	9

[‡‡] https://www.chemorbis.com/en/plastics-news/Asian-olefins-outlook-for-2024-Challenging-scenario-of-lackluster-derivatives-higher-feedstocks-an/2023/12/28/889612&isflashhaber=true#reportH (accessed 01.08.2024)

[§§] https://www.latibex.com/docs/Documentos/esp/hechosrelev/2024/Relat%C3%B3rio%20de%20Produ%C3%A7%C3%A3o%20e%20Vendas%20_1T24_ENG.pdf?iFPbLQ!! (accessed 01.08.2024).

Table 2. Raw material costs for alkenes in Asia and South America.[‡‡,§§]

Raw materials	Price in Asia, $/t	Price in South America, $/t
Ethane	230	143
Propane	660	439
Naphtha	667	671

In the future ethylene may even be available from such renewable source as bioethanol directing the 'dream reaction' onto the path of sustainable technological development. Along with the single-stage production of AA with simultaneous utilization of carbon dioxide, the accessibility of ethylene makes the implementation of this method extremely attractive and relevant especially for industry.

3. Development of AA synthesis

The search for a methodology for ethylene carboxylation has a long history spanning nearly 50 years. The main milestones of this journey are depicted schematically in Figure 2.

The initial stage of development led to the discovery of stable 3- and 5-membered Ni-lactones formed through the interaction of Ni-complexes with CO_2, including its insertion onto the C=C bond of coordinated alkenes. The importance and challenge of implementing the β-elimination process in the 5-membered Ni-lactone following its conversion into an acrylate moiety were recognized in the second stage. In the third stage a key transition was made from attempting to obtain AA itself to obtaining sodium acrylate. This stage can be considered the most eventful, with remarkable advancements made possible by accumulating data on the properties of catalytic systems, types of ligands, metals and bases suitable for the efficient synthesis of acrylate derivatives. At the same time parallel efforts were made to elaborate on the transfer of laboratory conditions to industrial technologies.

In the first stage, Aresta with co-workers[58] first synthesized and characterized a 3-membered Ni-lactone with η^2-CO-coordination of the CO_2 molecule, by performing its metal activation (Scheme 7). In this lactone, the degree of oxidation of Ni is not unambiguous. Based on the character of the complex formation and exchange reactions of neutral ligands — trialkylphosphine on CO_2, CO_2 on ethylene or hydrogen — one can conclude that Ni in it is in oxidation state (0). At the same time, the deviation from linearity of the coordinated CO_2 molecule suggests that it has some properties of $CO_2^{-\bullet}$, as well as nickel has properties of Ni(II), if we consider the formation of Ni–O and Ni–C bonds in intermediates formed during the interconversion of coordinated CO_2.[59,60] In nature, there is a close process of partial reduction of CO_2 to CO, proceeding with the participation of [NiFe]–CO-dehydrogenase[61] and being a

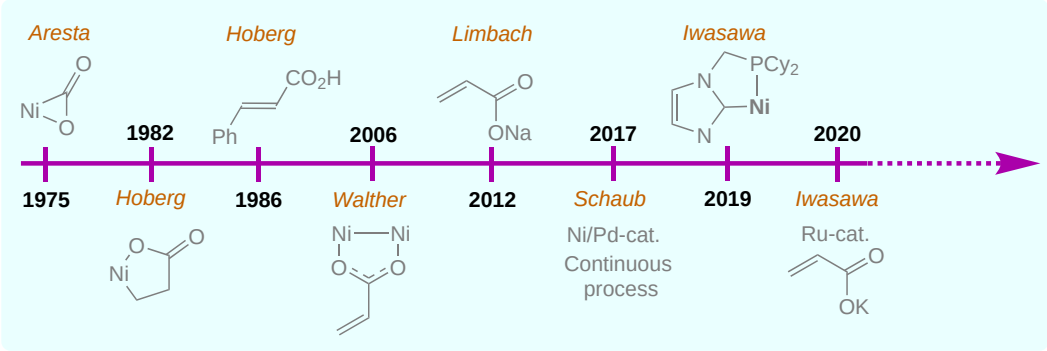

Figure 2. Significant dates in the development of AA synthesis.

Scheme 7

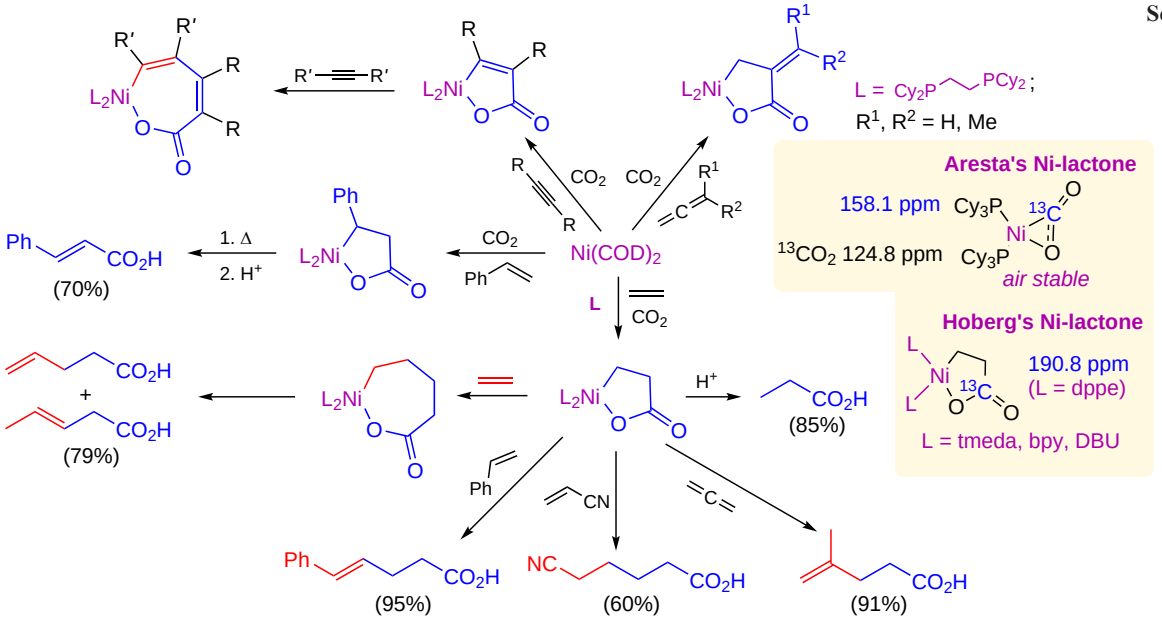

formal oxidative addition of the C=O bond (in CO_2) to nulvalent nickel. A characteristic feature of metallalactones, confirming their carboxylate nature is the chemical shift of the nuclei ^{13}C of the CO_2 fragment in NMR spectra, which is in the area of 160 ppm and higher, in contrast to free CO_2 with a shift of 124.8 ppm. Interestingly, η^2-CO-bound CO_2 shows itself as a good *O*-nucleophile, so it is easily protonated by acids.[59]

In 1982, Hoberg and Schaefer[62] synthesized a 5-membered Ni-lactone from $Ni(COD)_2$, norbornene, and CO_2 (1 bar), which laid the groundwork for numerous subsequent synthetic studies. Using other alkenes and acetylenes, Hoberg synthesized several Ni-lactones and explored their chemical properties in various stoichiometric transformations such as cycle expansion, acidic cleavage into carboxylic acids, ligand-exchange reactions, *etc*.[63–65] The synthesis of a 7-membered Ni-lactone from 1,3-diene was achieved by Walther and Dinjus during the same period.[66,67] However, all attempts to cleave Ni-lactone into acrylic derivatives were unsuccessful until 1986, when Hoberg discovered that Ni-lactone obtained from styrene could undergo *β*-H-elimination,[68] starting already at 85 °C and resulting in the formation of cinnamic acid (70%). By using complexes with DBU-ligands, he successfully carried out *β*-H-elimination in the seven-membered cycle to produce two isomeric pentenoic acids (79%) (see Scheme 7).[69] Over the next 20 years there was little progress in finding a solution to the problem of synthesizing AA itself. However, in 2006 Walther with co-authors,[70] made a significant breakthrough when they observed the formation of an acrylate κ,κ-*O*,*O*-complex (65%) for the first time. This complex was a binickel derivative with a Ni(I)–Ni(I)-bond formed using bis(diphenylphosphino)methane (dppm-ligand) (Scheme 8). The reaction involved the exchange of TMEDA-Ni-lactone for the dppm-ligand at 60 °C. Analysis of the reaction mechanism using deuterated lactone [(TMEDA)Ni(C_2D_4COO)] revealed that the *β*-elimination of deuterium (or hydrogen in the conventional lactone) was the rate-determining step. The authors proposed that through the exchange of phosphine ligands along with partial decarboxylation and deethenylation, a tris-phosphine — dppm-complex was formed, which together with the hydride complex produced the binickel product. Despite this discovery, the authors were unable to explain the origin of the intermediate hydride acrylate complex, which hadn't been obtained previously (see Scheme 8), and did not advance in this study.

Scheme 8

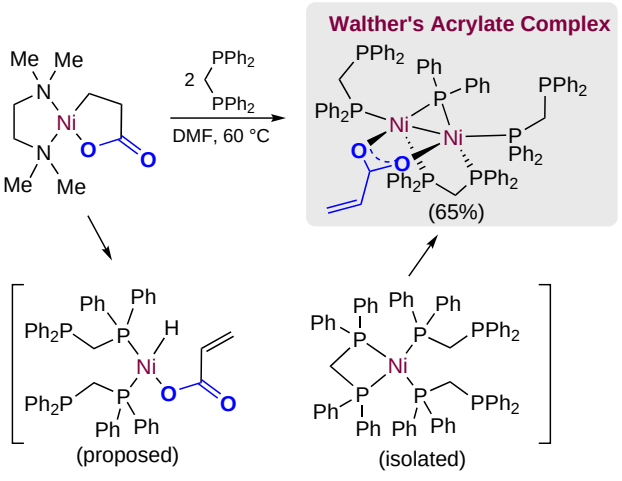

It became evident that the 5-membered Ni-lactone, being a highly stable cycle, requires additional stimuli for its transformation into AA. For example, internal stabilization of the C=C bond by the Ph-group, as seen in the cinnamyl derivative synthesized by Hoberg (see Scheme 7) or a decrease in the stability of the cycle itself, as in the 7-membered lactone. In this search for ways to target the transformation of Ni-lactone, Rieger with co-authors in 2010[71] suggested treating Ni-lactone with MeI to break the Ni–O bond. This idea proved successful, but methyl acrylate was only obtained in moderate yields (Scheme 9). It is assumed that the acyclic Ni-derivative undergoes a *β*-hydride shift more readily to form methyl acrylate, leading to Ni(0), which could then regenerate the Ni-lactone again under the influence of CO_2 and ethylene. A study on the synthesis of methyl acrylate from Ni-lactones with TMEDA, 1,2-bis(diphenylphosphino)ethane (dppe), 1,2-bis(diphenylphosphino)propane (dppp), 1,2-bis(diphenylphosphino)-butane (dppb) and pyridine, showed a dependence of methylation on the type of ligand.[72] Methyl acrylate was only formed with the first three ligands, with the highest yield achieved with the TMEDA-ligand (for 3 h and with 100 equiv. MeI) being 29% (40% according to IR spectroscopy or 56% according to NMR).

DFT calculations reveal that interaction of MeI with Ni-lactone results in the highest activation energy, leading to the formation of pentacoordinated Ni particles and a tricoordinated oxygen atom in the Ni–O bond in the transition state.

In a subsequent study by Limbach and Hoffmann with coauthors it was demonstrated[73] that Ni-lactone with the bulky 1,*2*-bis(di-*tert*-butylphosphino)ethane — dtbpe-ligand is preferentially methylated through the C=O-group, resulting in the opening of the lactone ring as the pathway with the lowest energy (Scheme 10). This methylation pathway was experimentally confirmed. Methylation with methyl triflate was conducted through the carbonyl group, followed by the exchange of the triflate anion with $[BAr^F_4]^-$ (BARF-anion). Treatment of the synthesized cationic complex, with Et_3N in CD_2Cl_2 produced a π-complex of methyl acrylate (15%) within 5 min. Newer data on quantum chemical calculations of the methylation mechanism, the impact of solvents, halogens in the methyl derivative, and other factors are discussed by Liu and co-workers.[74]

A new era in the study of Ni-lactones began after Limbach and co-workers[75] developed the catalytic synthesis of sodium acrylate. In 2007, Buntine with co-authors[76] demonstrated that a major challenge in obtaining AA through the 'dream reaction' was the unfavorable thermodynamic factors. Both in the gas phase (+57.4 kJ mol^{-1}) and in solution (+42.7 kJ mol^{-1}) the

Scheme 9

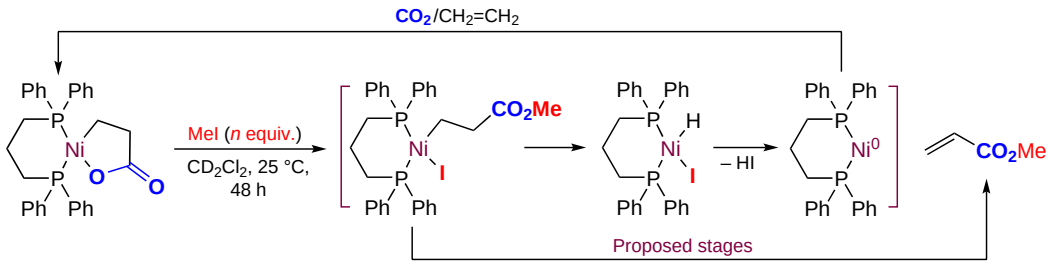

MeI, *n*	Yield
2	10%
10	16%
100	29%
Neat	33%

Scheme 10

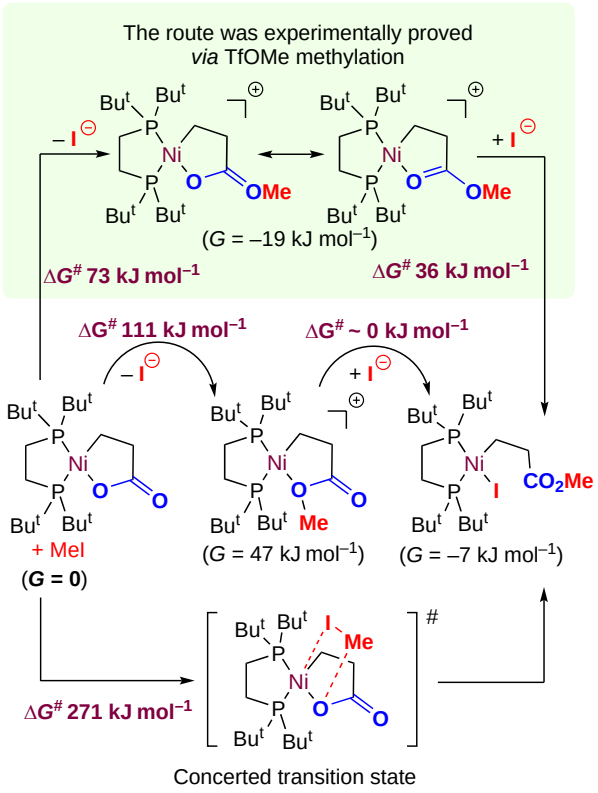

Scheme 11

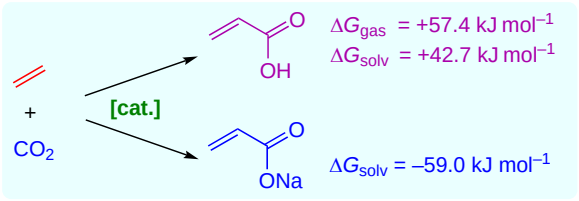

process is endothermic and does not proceed spontaneously (Scheme 11).

Upon synthesis of the methyl ester of AA, the thermodynamics are also unfavorable. Limbach suggested,[75] that converting the acid into the salt form could facilitate the reaction. In this case, the Gibbs energy changes its sign (–59 kJ mol^{-1}) and the reaction becomes thermodynamically feasible, with the final product — sodium acrylate — gaining significant energy. Bernskoetter with co-authors[77] studied the influence of the metal cation (Na^+) on the energy characteristics of the intermediates in the preparation of acrylate. They showed that the presence of the sodium cation and the formation of salted forms with it reduce the energy of all intermediates (Fig. 3). According to Bernskoetter's DFT calculations, there are four intermediates in addition to γ-lactone on the reaction coordinate. These include agostically bound γ- and β-*H*-intermediates, acrylate coordinated to Ni-hydride, and β-lactone with a 4-membered cycle. Under normal conditions, the transformation to Ni-hydride acrylate and β-lactone results in a positive charge on the Ni atom and a negative charge on the carboxyl group with the energies of such intermediates being as high as up to 117.6 kJ mol^{-1}. The interaction of γ-lactone with sodium cations (as a trimolecular THF solvate) significantly decreases the relative energy (from 21.6 to 37.1 kJ mol^{-1}) for the high-energy intermediates. Furthermore, the *Na*-β-lactone is found to be 9.77 kJ mol^{-1} more stable than the original *Na*-γ-lactone. XRD data confirm the weakening of the Ni–O bond in the complex with $NaBAr^F_4$ (the Ni–O bond length increases by 0.057 Å). NMR spectra indicate that this complex shifts into equilibrium with *Na*-β-lactone when heated to 45–78 °C, but its content remains in the range of 25–33%, meaning experimentally its energy is higher than that of *Na*-γ-lactone.

In general, the calculated data from Bernskoetter[77] align well with the experimental results from Limbach.[75] Limbach studied the impact of bidentate phosphine ligands (dppm, dppe, dppp, dtbpm, dtbpe and dtbpp) on the formation of Ni-lactone from CO_2 (6 bar) and ethylene (2 bar). Among the ligands tested, lactone formation was only observed with dtbpe (35%) and dtbpm (60%). Additionally, the Ni-lactone with the dtbpm-ligand immediately decomposes back into the initial gases upon pressure decrease. In contrast, the lactone with dtbpe remains stable and can be stored in an inert atmosphere for several months without any changes.

However, when Bu^tONa is used, the dtbpe-Ni-lactone easily transforms into an η^2-C,C-complex of sodium acrylate in a high yield (Scheme 12). The release of the reaction product, sodium acrylate, is catalyzed by ethylene in the catalytic cycle. The authors successfully conducted an 18-fold recycling of the entire process and achieved TON = 10. The acrylate TON was measured by NMR in D_2O solution using an internal standard.

Quantum chemical modeling for systems using strong bases such as Bu^tONa or MeONa as shown by Limbach[75] revealed that the sodium ion coordinates to the carbonyl group of the lactone, activating it. However, for an alkoxylate with a quaternary ammonium cation, this process does not occur. This finding is consistent with the data presented by Bernskoetter.[77] In a DFT study Limbach also demonstrated that the transformation of lactone in the presence of alcoholate (with an alcoholate cluster coordinated through Na) is more likely to occur through the simultaneous abstraction of the α-proton adjacent to the carboxyl group and the formation of a π-complex with sodium acrylate. The authors do not rule out the involvement of the alkoxide anion in the Ni–O bond breakage of the lactone, but note that the process of β-hydride elimination requires high activation energies.

Scheme 12

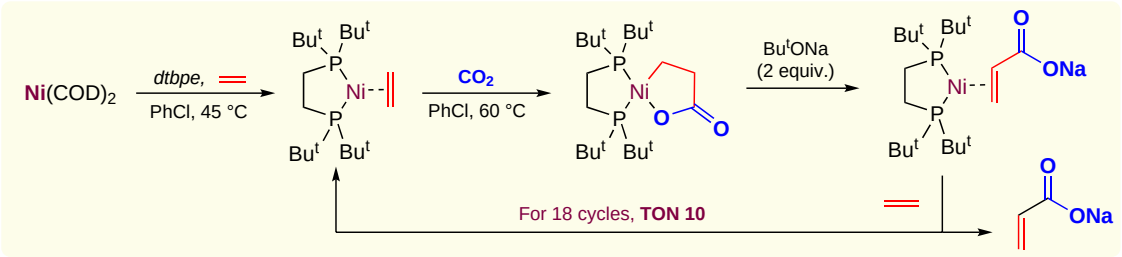

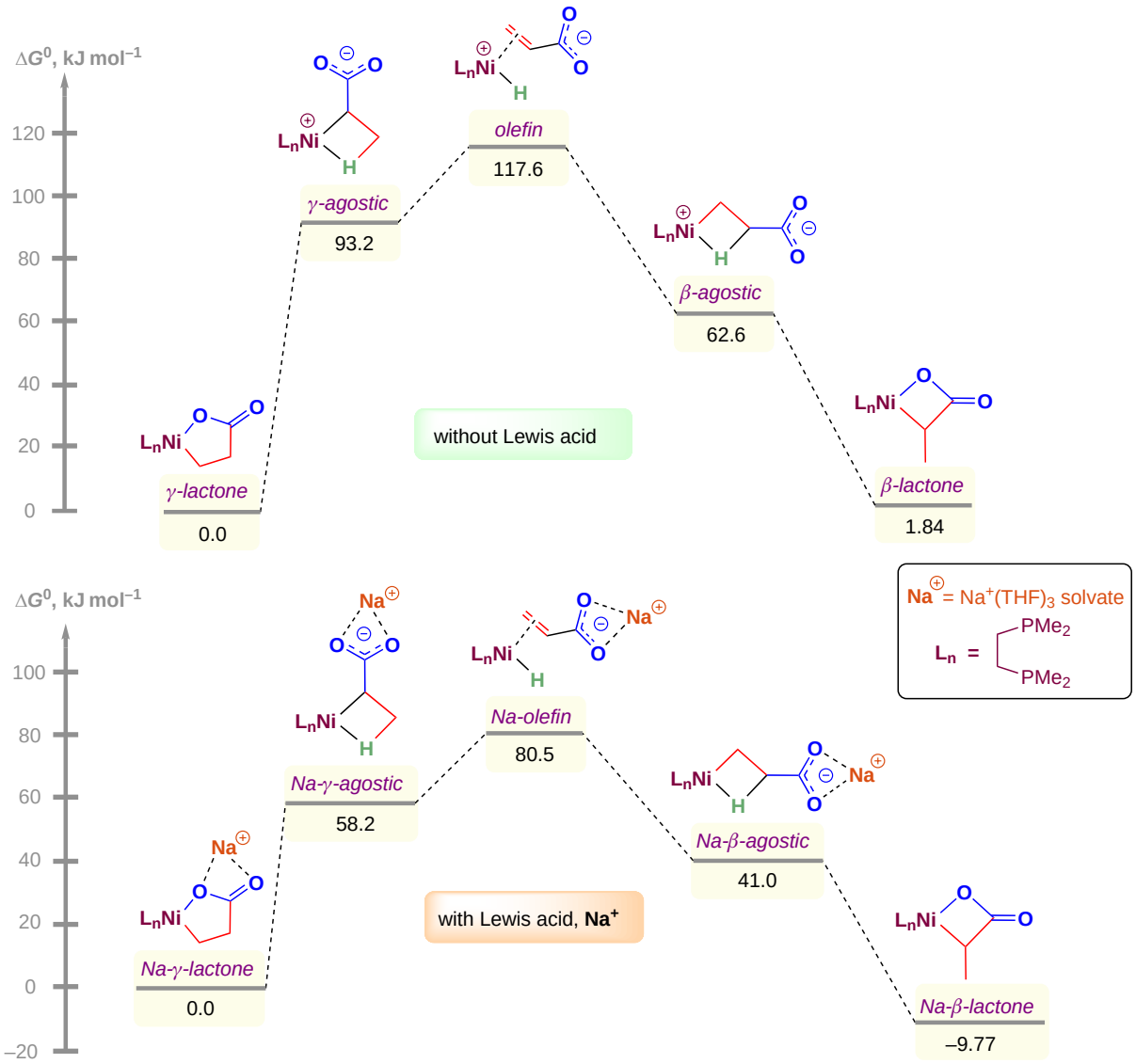

Figure 3. DFT calculations of Ni-lactone transformation without and in the presence of Na cations.

However, the step-by-step procedure of catalyst recycling developed by Limbach, involving pressure relief, changing the type and composition of gases turned out to be so complicated that Vogt and co-workers[78] noted the impracticality of this approach. They proposed using lithium salts as stronger Lewis acids to facilitate all stages of Ni-lactone transformation (Scheme 13). According to DFT calculations, when using a system with a weak base (triethylamine) and lithium iodide, the *β*-H-elimination process appears to be preferred. The role of the base, according to the authors, likely facilitates the reductive elimination of HI.[78] In this case, lithium ions facilitate the entire process of *β*-H-elimination by 20 kJ mol^{-1} better than sodium ions. The authors confirmed their idea experimentally; the transformation of dppe-Ni-lactone into lithium acrylate (73%) with 5 equiv. LiI proceeds without a base, although the addition of 50 equiv. Et_3N increases the yield of acrylate up to 95%. The addition of Zn improves the activity of the catalyst but is not essential, while in the absence of LiI the reaction totally fails. Under optimal conditions with dcpp-ligand (1,3-bis(dicyclohexylphosphino)propane) and an ethylene pressure of 25 bar, the TON of the reaction was 14–21. The authors also noted the formation of by-products that reduced the catalysis efficiency.

Limbach with co-workers[79] also updated the initial synthesis conditions, which involved replacing the base and ligand (Scheme 14). The need to replace the base was explained by the fact that alcoholates and strong basic amines (like DBU) are irreversibly neutralized by CO_2, while phenolates react reversibly with CO_2 due to their lower nucleophilicity. This behavior of phenolates was already known from the Kolbe–Schmitt carboxylation reaction of phenolates. Using sodium 3-fluorophenolate, phosphine ligands were screened, and although the BenzP*-ligand was not the most active at 80 °C (DuanPhos, TangPhos ligands were more efficient), it became the most productive at higher temperatures. Optimization of all parameters led to relatively high TONs of sodium acrylate. The most efficient were 3- and 2-fluoro-substituted sodium phenolates, with TON reaching 35 at 100 °C, although further temperature increases had a negative impact. Increasing the amount of base to 100 equiv. had little significance, while adding the reducing agent Zn and increasing pressure produced a stronger effect — 300 equiv. of base and 100 equiv. of zinc with a doubled gas pressure resulted in the highest value of TON = 107. The catalytic process showed high efficiency not only in the reaction with ethylene, but also with other alkenes (see Scheme 14). Significantly high values of TON = 75–116

Scheme 13

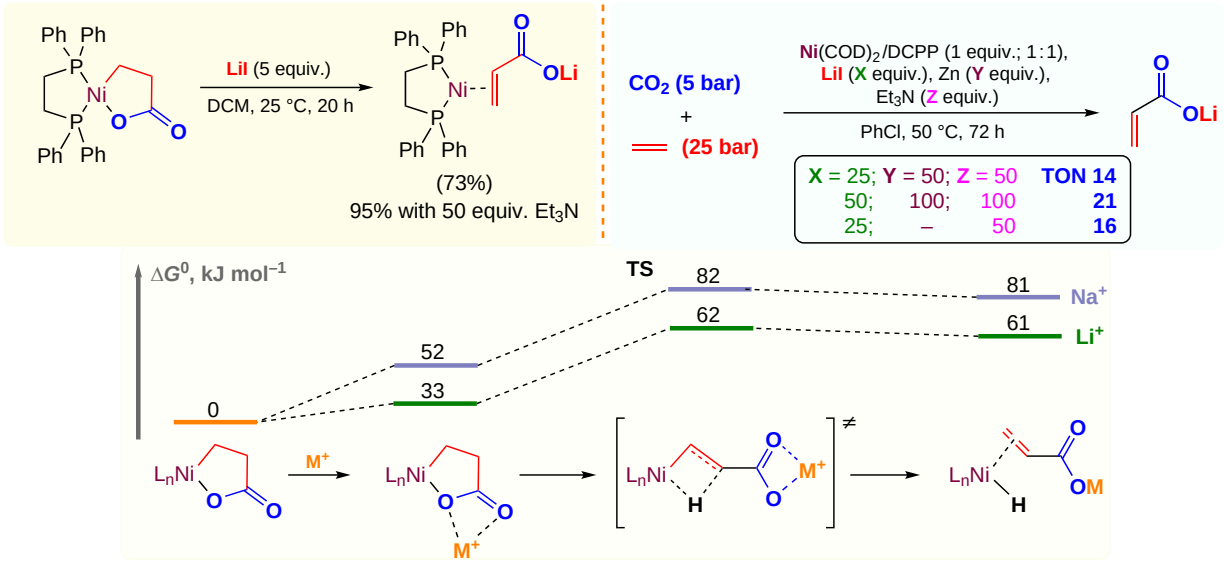

Scheme 14

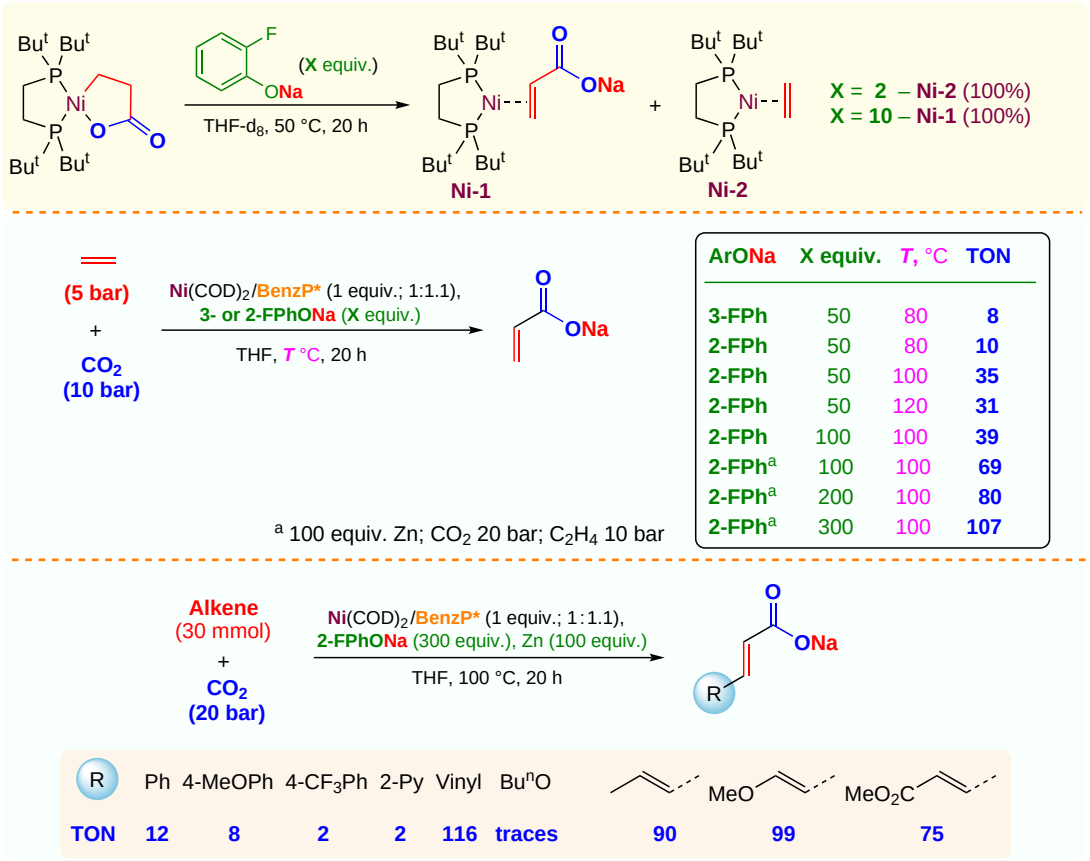

were obtained with vinylic derivatives almost regardless of the electronic character of the substituents with the C=C bond of the alkene.

Bernskoetter and co-workers,[80] noting the presence of chiral centers in the BenzP*-ligand as an unnecessary and complicating factor, proposed the use of a symmetric achiral analogue — Pr^{i}BenzP-ligand (Scheme 15). However, the synthesized Pr^{i}BenzP showed worse results — TON = 45 compared to 82 with BenzP*. The LiI additive revealed an inhibitory effect (TON = 14 and 30), while Zn additive was favorable in both cases (TON = 84 and 109). The most interesting finding was the use of the less basic sodium 2-chlorophenolate, which was ineffective with Pr^{i}BenzP (TON = 30), but surprisingly increased the catalyst activity (TON = 135) in the presence of BenzP*. Furthermore, with NaI additive the TON value was significantly increased to previously unattainable levels (TON = 404). Actually, the role of each additive is not fully elucidated, as the authors point out, due to 'there exist multiple interactions between the Zn reductant, Lewis acidic salts, phenoxide bases, and nickel species employed in these catalytic systems'.[80]

Scheme 15

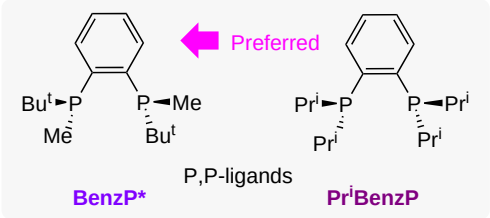

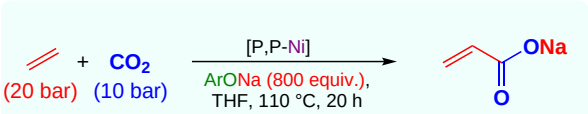

[P,P-Ni]	ArONa	LiI	NaI	Zn	TON
PriBenzP	3-FPh				45
BenzP*	3-FPh				82
PriBenzP	3-FPh	100			14
PriBenzP	3-FPh	100		200	30
PriBenzP	3-FPh			200	84
BenzP*	3-FPh			200	109
PriBenzP	2-ClPh			200	30
BenzP*	2-ClPh			200	135
PriBenzP	2-ClPh		100	200	30
BenzP*	2-ClPh		100	200	404

Seeking more information on the structure-activity relationship (SAR) of previously synthesized BenzP-type ligands, Bernskoetter with co-workers[81] performed a joint screening of ligands and phenolate bases. However, despite their efforts, they were unable to propose an approach to selecting ligands and bases that would allow for the directed design of catalytic systems. For diphosphine Ni complexes, they only proposed a model of coordination sphere quadrants suggesting that the optimal characteristics are found in a BenzP-ligand with alternating hindered and freer quadrants. In this study, the researchers obtained data on the TON of the catalyst dependence on the electronic and steric characteristics of the phenolate base (Scheme 16). A comparison of the properties revealed the need for a balance of factors: good basicity to facilitate proton cleavage in the Ni-lactone or intermediate particles, and a certain steric environment to maintain access to the Ni-complex while limiting the stability of the carbonate formed during the reaction from sodium phenolate. Experimental data in Scheme 16 illustrate the accumulation of acrylate (dashed line) with sodium 3-fluorophenolate, as well as carbonate accumulation and phenolate consumption. It is evident that after just 10 hours, the reaction is nearly halted, though the addition of a new portion of phenolate (not shown in Scheme 16) reactivates the catalysis.

Previously, Schaub and co-workers[82] conducted a study on the decomposition temperature of carbonates of various bases using the TGA method (Scheme 17). In their study typical phenolate carbonates, that are active in the synthesis of sodium acrylate, decomposed into CO_2 and alcoholate at moderate temperatures ranging from 50 to 70 °C. These temperatures were lower than those required for the catalytic reaction. On the other hand, inactive bases like sodium methylate and sodium ethylate, produced carbonates that were too stable to decompose even at temperatures as high as 330 °C.

Scheme 17

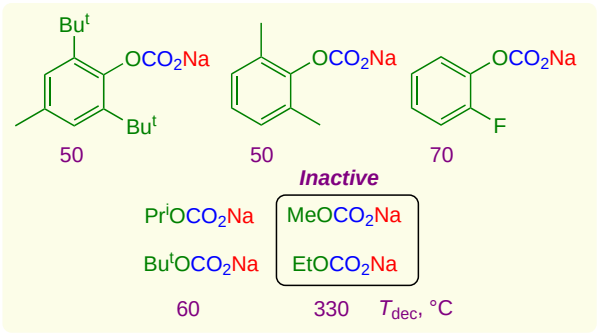

To determine if the thermal stability of carbonates changes in real conditions under CO_2 pressure and in the presence of a solvent, the authors conducted tests on the decomposition of sodium *tert*-butyl carbonate in an autoclave. The decomposition process was monitored using an integrated IR sensor. The results indicated that the decomposition temperatures were almost identical to those measured under standard conditions. These findings provide insight into why hindered phenolates (see Scheme 16) are more effective as bases.

One reason for the limited reactivity of Ni-catalysts is their oxidation and disproportionation. Therefore, Zn powder is often added to the reaction as a reducing agent. While all authors suggest that Zn enables the reduction of Ni^{2+} complexes to Ni^0, its participation in the catalytic cycle or mechanisms of deactivation are not clearly indicated.

Iwasawa and co-workers[83] set a goal to enhance the stability of Ni-complexes in the synthesis of acrylates. They selected carbene-phosphine-type ligands (NHC-P) because, thanks to the

Scheme 16

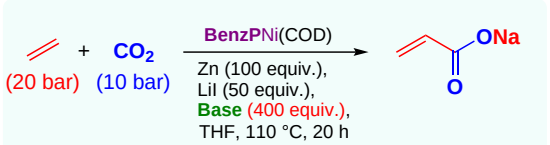

Base	pKa	TON
HMDSNa	26	⩽1
ButONa	19.20	7
2,6-But2-4-MePhONa	12.20	88±8.5
2,6-Pri2PhONa	11.10	174±9.2
2-Cl-6-MePhONa	9.71	111±2.1
3-FPhONa	9.29	105±9.9
2-ClPhONa	8.56	158±9.5
2,6-Cl2PhONa	6.79	32±9.9

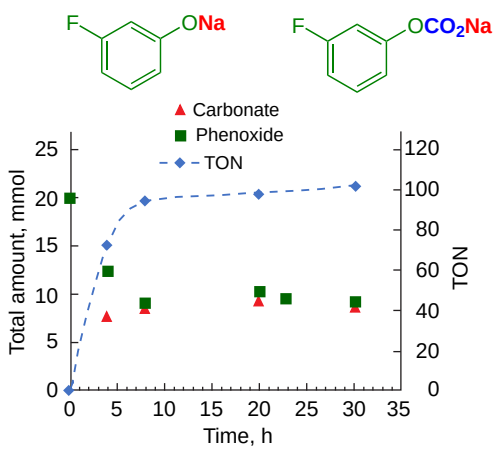

Scheme 18

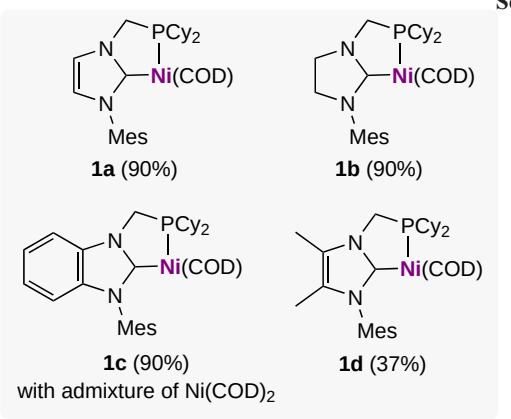

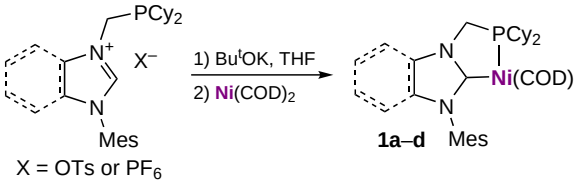

[NHC,P–Ni]	Additive, X eq.	*T*, °C	TON
1a	–	100	6.9
1a	–	120	34
1a	–	145	58
1a	Zn, 100	145	73
1a	AcONa, 300	145	94
1a	BzONa, 300	145	12
1a	TFAONa, 300	145	31
1b	AcONa, 300	145	2.3
1c	AcONa, 300	145	3.2
1d	AcONa, 300	145	140
1d	AcONa, 1200[a]	145	450

[a] MesONa (1200 equiv.)

NHC-fragment, they also have a higher donor ability (Scheme 18).

Complexes **1a–d** were prepared from imidazolium salts by sequential treatment with Bu^tOK and then $Ni(COD)_2$ in THF. The synthesis of Ni-lactone from ethylene and CO_2 with **1a**, proceeds within 30 min, whereas the analogous process with dcpe-ligand requires several days. Due to its asymmetric structure, Ni-lactone is obtained as a mixture of spatial isomers. Measurement of the oxidizing potential of **1a** (–1.26 V), showed that its reducing ability is significantly higher than that of [Ni(dcpe)(cod)] (–0.95 V). Test experiments of *β*-H-elimination in lactone with Bu^tOK and ligand exchange of potassium acrylate for ethylene showed good results. Screening of catalysts and conditions for acrylate synthesis revealed a new efficient base for use with the above complexes — sodium mesitolate (MesONa). Apparently, due to the need for a high temperature of 145 °C (lower temperature reduces the yield) to achieve acceptable activity, other phenolates are of little use as they undergo carboxylation by the Kolbe–Schmitt reaction. The addition of sodium acetate together with complex **1a** significantly increases the TON value to 94 versus 58 without addition. The maximum efficiency was shown by catalyst **1d** (TON = 140), with a decrease in catalyst loading leading to an increase in the TON value to 450, an unprecedented value, thus showing efficiency and adaptability to the conditions for the synthesis of NHC,P-ligands. Interestingly, catalysts **1b**,**c** of close structure were completely inefficient.

Hong and co-workers[84] continued the study of NHC-ligands and synthesized a series of stable NHC,N-ligands **2a–f** based on imidazo[1,5-*a*]pyridine (Scheme 19).

Despite the different substituents in the pyridine and imidazole moieties, the efficiency of such complexes in the synthesis of AA salts remained low at the investigated temperature (TON = 0.34–8.45) and did not exceed the activity of standard nickel diphosphine complexes (TON = 9–14) tested for comparison.

When applying photoactivation to the developed NHC,P systems, Iwasawa and co-workers[85] unexpectedly obtained a salt of methylmalonic acid instead of AA (Scheme 20).

Earlier in 1991 Hoberg and co-workers demonstrated[86] that a stoichiometric reaction is feasible with Ni-lactone, albeit

Scheme 19

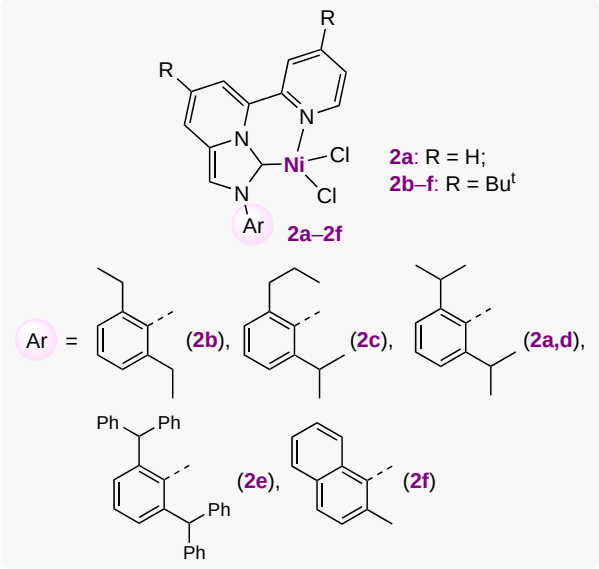

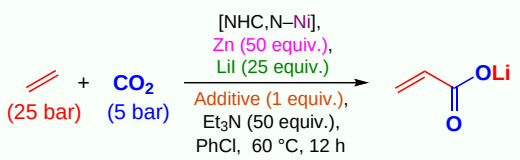

[NHC,P–Ni]	Additive	TON
2a	–	0.34
2b	–	0.85
2c	–	1.08
2d	–	0.80
2e	–	0.62
2f	–	0.50
2a	PCy_3	1.80
2b	PCy_3	6.77
2c	PCy_3	7.28
2d	PCy_3	8.45
2e	PCy_3	8.14
2f	PCy_3	1.94

Scheme 20

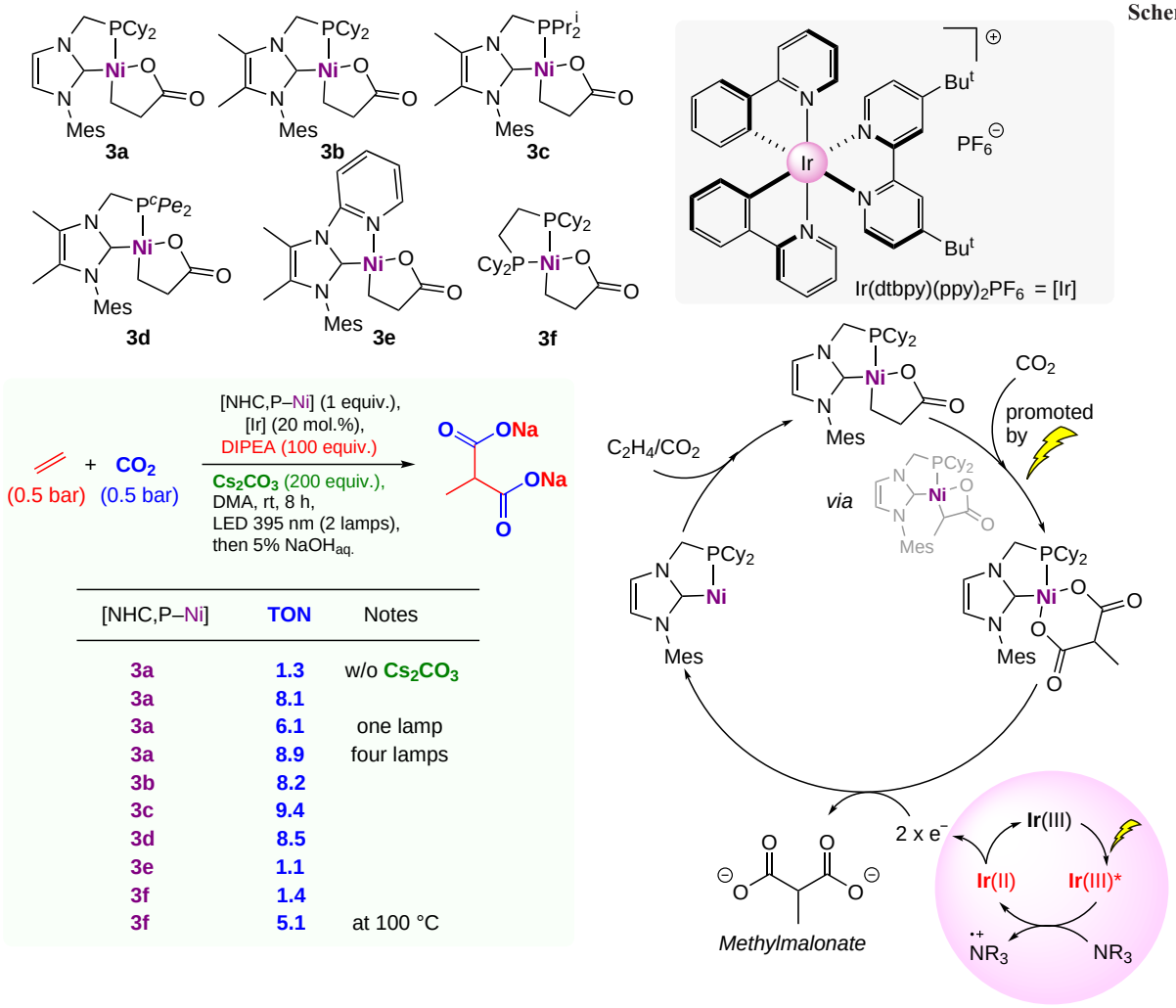

[NHC,P–Ni]	TON	Notes
3a	**1.3**	w/o Cs_2CO_3
3a	**8.1**	
3a	**6.1**	one lamp
3a	**8.9**	four lamps
3b	**8.2**	
3c	**9.4**	
3d	**8.5**	
3e	**1.1**	
3f	**1.4**	
3f	**5.1**	at 100 °C

requiring the presence of $BeCl_2$ (10 bar CO_2, 70 °C, THF/Py, 1 : 1) through the formation of a four-membered lactone, while the yield of methylmalonic acid is 50%. In a subsequent study, Iwasawa conducted[85] a photocatalytic synthesis using a 1 bar CO_2/ethylene (1 : 1) mixture in DMA solution with 20 mol% Ir(dtbpy)(ppy)$_2$ PF_6 and irradiated with 395 nm LED lamps. The optimal conditions included the use of 2 lamps, Cs_2CO_3 additive (200 equiv.) and the reducing amine (or 'sacrificial' amine) DIPEA (100 equiv.). Under these conditions, the NHC,P-complexes exhibited the TON values as follows: **3a** — 8.1, **3b** — 8.2, **3c** — 9.4 and **3d** — 8.5, showing close values. The proposed mechanism of this reaction involves the photoinduced insertion of CO_2 into the 4-membered Ni-lactone with an alpha-methyl group formed through isomerization, resulting in a malonate Ni(II) derivative. It is worth noting that in Iwasawa's[85] work, the NHC,N-ligand was one of the least active in catalysis, comparable in activity to the diphosphine dcpe-ligand.

Along with the target coupling reaction and the productive cycle of the Ni-catalyst, there are several side processes associated with the removal of Ni-complexes from the catalytic cycle of acrylate formation. These processes have been analyzed in Limbach's work (Scheme 21).[23] The main products associated with the occurrence of side processes and reduced catalyst activity in the target reaction include: 1) Ni^0 bis-phosphine complexes; 2) a 3-membered lactone as an intermediate for the competitive coordination of CO_2 with ethylene and Ni *via* η^2-type coordination followed by oxidative transformation to nickel carbonate or precipitation of metallic nickel; 3) a 7-membered lactone formed by sequential double introduction of ethylene; 4) a 4-membered lactone obtained by isomerization of a 5-membered lactone, which can form a malonate complex upon introduction of a second CO_2 molecule. Oxidation of phosphine by coordinated CO_2 is also a side process.[60]

Since Ni-based catalysts do not achieve high TON values and require large excesses of base, reducing agent or other additives to increase stability and achieve meaningful activity in the catalytic cycle, the interest in using other metals is of both fundamental and practical importance. Indeed, the carboxylation reaction of ethylene to form metallalactone or acrylate can proceed in the presence of many other metals,[87] such as Ti,[88] Zr,[89] V,[90] Mo and W,[91–93] Fe,[94–96] Ru,[97] Rh,[98,99] Pd,[100] Co[101] and Al.[102] However, the successful realization of the catalytic reaction is only possible in some systems.

One of the first metals used for catalytic carboxylation of alkenes along with nickel was palladium. Inoue (1976)[103] and Musco (1978)[104] observed the formation of carboxylated telomers from 1,3-butadiene and CO_2 in the presence of phosphine complexes of Pd, including 5- and 6-membered unsaturated lactones.

Limbach and co-workers[100] applied Pd-catalysts in the synthesis of acrylate (Scheme 22). They were able to obtain a Pd-lactone for the first time, which was formed as a mixture (1 : 1) with an acrylate complex through the lactonization of η^2-coordinated AA. The pure lactone was then isolated through

Scheme 21

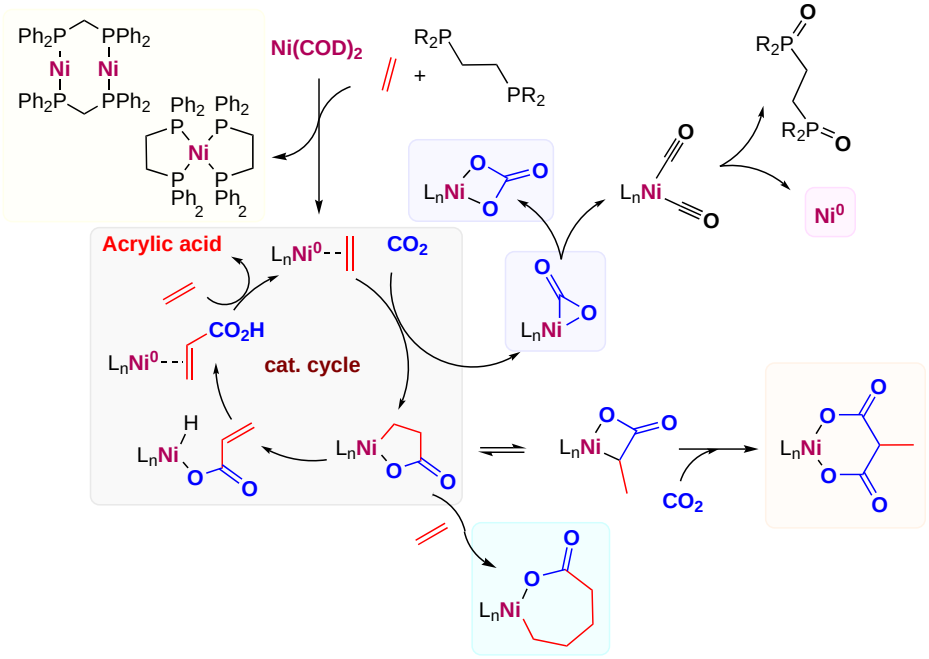

crystallization. Various Pd complexes were tested for the catalytic synthesis, with $(COD)PdCl_2$ and $(\eta^5\text{-Cp})Pd(\eta^3\text{-allyl})$ showing greater activity. The latter complex did not require a reducing agent (Zn). Synthesis conditions for the acrylate were screened using a commercially available $(COD)PdCl_2$. The maximum TON = 29 was achieved when the catalyst loading was reduced by half (0.5 mol.%) from standard conditions (1.0 mol.%), with TON values of 24 (145 °C) and 27 (120 °C). In addition to ethylene, 1,3-butadiene and 1,3-pentadiene readily enter the carboxylation reaction with the catalyst loading of 0.33 and 1.0 mol.% and TON values of 24 and 50, respectively.

In the same year, Schaub and co-workers [105] presented an extensive study dedicated to improving catalytic synthesis conditions and increasing TON values on both Pd and Ni catalysts. This work also aimed to explore catalyst recycling (Table 3).

Initial screening of phenolate bases showed that the 2-methyl- and 2,6-dimethyl derivatives allowed relatively high TONs to be achieved with Pd- (TON = 38) and Ni-catalysts (TON = 69) in the presence of a dcpe-ligand, but a temperature of 145 °C was required. The lipophilic sodium 2,6-dimethyl phenolate was also considered a better base for the continuous process, where the sodium acrylate should be separated by aqueous treatment in a two-phase system with phenolate regeneration through an organic solvent. The authors were able to reduce the amount of Zn-reductant to 5 equiv. and show that even in its absence the catalysts continue to work, but the reduction in TON could not be avoided. However, as Schaub points out, the need to introduce a reducing agent adds complexity and cost to the process. These tests revealed that the nulvalent palladium complex $Pd(PPh_3)_4$ without the addition of Zn has acceptable productivity characteristics (TON = 28). Furthermore, a suitable solvent such

Scheme 22

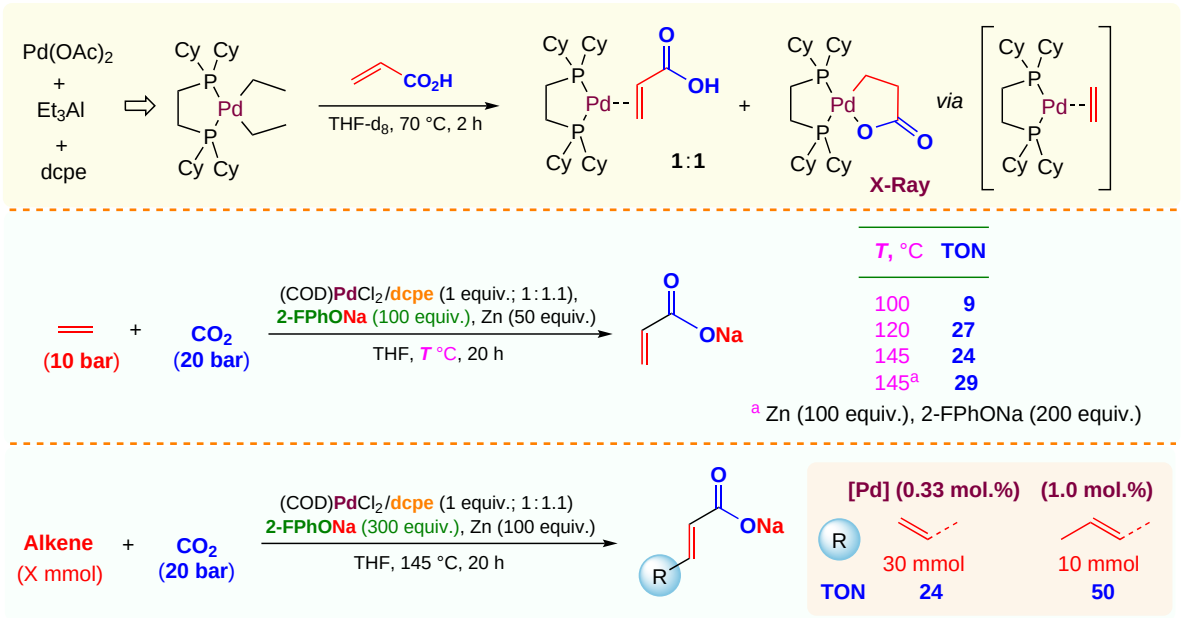

Table 3. Conditions for Pd- and Ni-catalyzed synthesis of sodium acrylate.[105]

	Base (100 equiv.); **Zn (50 equiv.)** THF, 20 h, ethylene (10 bar), CO_2 (20 bar)		
Base	$(COD)PdCl_2$/dcpe/ 145 °C	$Ni(COD)_2$/BenzP*/ *T*, °C	
	TON		**TON**
2-F-PhONa	**24**	120 °C	**107**
2,6-diF-PhONa	**1**	80 °C	**1**
2-Me-PhONa	**31**	80 °C	**4** (150 equiv.)
2,6-diMe-PhONa	**8**	80 °C	**4** (150 equiv.)
		145 °C	**43** (150 equiv.)
		dcpe/145 °C	**69** (150 equiv.)
Zn (экв.)	**2,6-diMe-PhONa** (100 equiv.); dcpe (1.1 equiv.), 145 °C, THF, 20 h, ethylene (10 bar), CO_2 (20 bar)		
	$(COD)PdCl_2$	$Ni(COD)_2$	
Zn (5 equiv.)	**29**	**56**	
Zn (0 equiv.)	**21**	**55**	
[Pd]	**2,6-diMe-PhONa** (100 equiv.); dcpe (1.1 equiv.), 145 °C, THF, 20 h, ethylene (10 bar), CO_2 (20 bar)		
$Pd(OAc)_2$	**11**	–	
$[Pd(allyl)Cl]_2$	**14**	–	
Pd(Cp)(allyl)	**18**	–	
$Pd(dba)_2$	**0**	–	
$Pd(PPh_3)_4$	**28**	–	
Solvent	**2,6-diMe-PhONa** (100 equiv.); dcpe (1.1 equiv.), **Zn (5 or 0 equiv.)**, 145 °C, **Solvent**, 20 h, ethylene (10 bar), CO_2 (20 bar)		
	$(COD)PdCl_2$/Zn	$Ni(COD)_2$	$Pd(PPh_3)_4$
THF	**29**	**55**	**28**
Anisole	**45**	**44**	**43**
Anisole (wet)	**39**	**22**	**40**
Bu^nOPh	**6**	**47**	**0**
$(Bu^nOCH_2)_2$	**1**	**3**	**23**
Base	**Base** (50 equiv.); dcpe (1.1 equiv.), **Zn (1 equiv.)**, **Anisole**, 20 h, ethylene (10 bar), CO_2 (20 bar)		
	$(COD)PdCl_2$/Zn	$Ni(COD)_2$	$Pd(PPh_3)_4$
2,6-diMe-PhONa	**39**	**44**	**40**
2,6-diPr^i-PhONa	**24** (100 equiv.)	**46**	**35**
2,6-diBu^t-PhONa	**4** (100 equiv.)	**17**	**20**
2,6-diBu^t-4-Me-PhONa	**7** (100 equiv.)	**33**	**50**
2,6-diBu^t-4-Me-PhONa	–	–	**106** (1000 equiv.)

as anisole was identified to ensure compatibility with the catalytic system and immiscibility with water during the acrylate extraction and catalyst regeneration step. Moreover, only in the case of $Pd(PPh_3)_4$, almost no drop in catalyst productivity was observed when switching from fresh dry anisole to wet solvent in the recycling step. The phenolic base structure was also optimized to avoid phenol loss during the acrylate separation step. The best TON = 50 was obtained with 2,6-diBu^t-4-MePhONa, whose conversion was almost quantitative (99%) and its loss resulting recycling was only 0.6%.

A crucial step in the recycling procedure of the catalytic process was washing the product and excess base with water to remove the catalyst and ligand, which remained in the organic layer. Table 4 provides a summary of the TON values for the first and second catalyst cycles. Despite conducting all manipulations of the second cycle in an inert atmosphere, the catalyst's activity decreased significantly.

The addition of a reducing agent was necessary to maintain acceptable activity in the second cycle, indicating oxidation of the complexes during the product separation manipulations. Furthermore, the TON values still remained several times lower than in the first cycle. Through extensive screening of catalytic synthesis conditions, Schaub was able to develop a more efficient system for the synthesis of sodium acrylate, though it was still far from practical use.

Schaub further demonstrated[82] that an appreciable efficiency (TON = 50) can be achieved with $Pd(PPh_3)_4$ using Bu^tONa (50 equiv.), while the potassium and lithium salts yield lower TON values, showing 41 and 33, respectively. *tert*-Butylate has a significantly lower molecular weight compared to substituted phenolates, allowing for a higher concentration of base in the reaction medium of 0.66 M (20 mmol), resulting in a TON = 88. By reducing the catalyst loading (to 1.0 μmol) the maximum TON value of 100 was achieved in 65 h. It is important to note that the simultaneous catalyst deactivation process hinders the TON value from increasing proportionally to the decrease in catalyst loading. The carboxylation of various alkenes was screened under optimized conditions (Scheme 23). Notably, 1,3-butadiene showed exceptional reactivity, completing the reaction within 3 h at 100 °C compared to standard conditions of 20 h at 145 °C, surpassing previous reactivity achieved with Ni-catalyst. The carboxylation of styrene followed a similar pattern to Ni-systems. Propylene and hexene-1 produced a mixture of linear and branched products (l/b), with propylene carboxylation demonstrating high efficiency for the first time. The crotonate/methacrylate ratio for propylene was 1.4, while the ratio of the corresponding products for hexene-1 was 3.3. Cyclic acrylates were obtained with low TON values (see Scheme 23).

Assuming that the Pd-acrylate complex can agglomerate in low-polarity solvents like anisole, Schaub with co-authors[106] used amide solvents (Scheme 24, DBF, *N*,*N*-dibutylformamide; NMP, *N*-Me-pyrrolidone; CHP, *N*-cyclohexylpyrrolidone), which are much more compatible with the developed catalytic

Table 4. Tests[a] on recycling with the addition of a fresh portion of base and Zn (in parentheses).[105]

No.	Catalyst	Base, mmol	Zn, mmol	TON 1	TON 2
1	$(COD)PdCl_2$	2,6-diMe-PhONa, 20 (+20)	1 (+1)	55	15
2	$Pd(PPh_3)_4$	2,6-diBu^t-4-Me-PhONa, 10 (+10)	0 (+0)	50	1
3	$Pd(PPh_3)_4$	2,6-diBu^t-4-Me-PhONa, 10 (+10)	0 (+1)	50	18
4	$Ni(COD)_2$	2,6-diMe-PhONa, 10 (+10)	0 (+0)	44	0
5	$Ni(COD)_2$	2,6-diMe-PhONa, 10 (+10)	0 (+1)	44	10

[a] Conditions: [Pd] (0.1 mmol), dcpe (0.11 mmol), anisole (30 mL), ethylene (10 bar), CO_2 (20 bar), 145 °C, 20 h.

Scheme 23

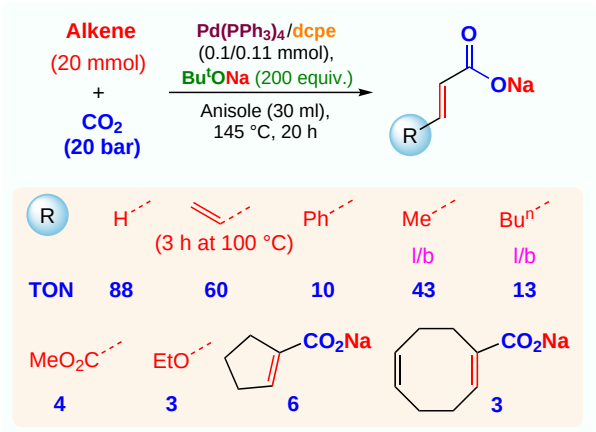

system. These solvents not only stabilize the catalytically active Pd species, but also dissolve CO_2 better. In contrast to anisole, increasing the CO_2 pressure from 20 to 40 bar in amide solvents significantly increases activity, and the combination with Bu^tONa makes the reaction even more efficient. The TON value reaches 152, and when the catalyst loading is reduced by a factor of 10 (0.01 mmol) it reaches 514 (for 5 h TON = 307, TOF = 61 h^{-1}). For anisole, the TOF value for 15 h was only 5 h^{-1}. These activity values were unattainable earlier and are promising for the development of an industrial synthesis scheme. At the same time the reuse of the catalytic system even increases its activity (Table 5). Furthermore, the success of the developed system is evident in the 100% conversion rate of the base, along with the option to utilize the more technologically advanced and cost-effective Pr^iONa, albeit with lower efficiency in the initial stage.

Scheme 24

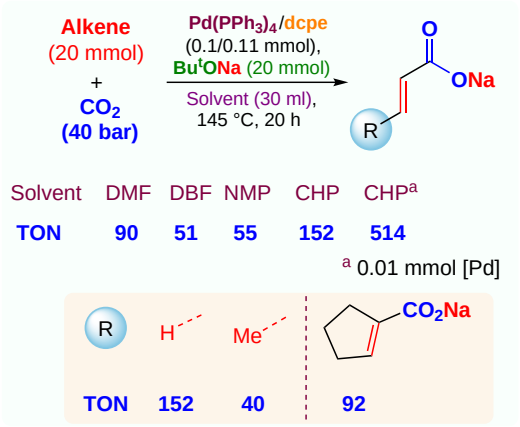

Table 5. Tests[a] for recycling using amide solvents.[106]

No.	Base, mmol	[Pd], mmol	Solvent	TON 1	TON 2
1	Bu^tONa, 25 + 25	0.2	DBF	135	100
2	Pr^iONa, 15 + 15	0.2	DBF	30	100
3	Bu^tONa, 15 + 15	0.1	CHP	78	90
4	Pr^iONa, 15 + 15	0.1	CHP	30	100

[a] Conditions: [$Pd(PPh_3)_4$] (1 equiv.), dcpe (1.1 equiv.), solvent (30 mL), ethylene (10 bar), CO_2 (40 bar), 145 °C, 20 h.

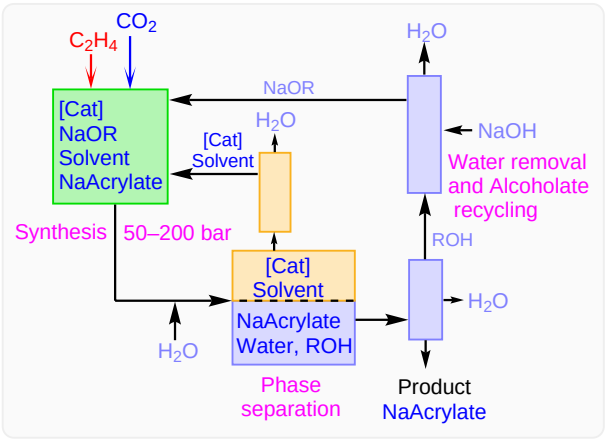

Figure 4. Process flow diagram for the synthesis of sodium acrylate.

The authors have proposed an optimized process flow diagram for the continuous synthesis of sodium acrylate. This diagram takes into account the separation of the reaction product by water, as well as the regeneration of alcoholate and catalyst solution in an amide solvent. Additionally, provision is made for the removal of traces of water from the solvent under mild vacuum conditions (Fig. 4).

In this way the use of amide solvents improved both the catalytic activity and facilitated the recycling of the entire reaction mass. The achieved TON value >500 combined with the use of inexpensive and readily available bases provides a solid foundation for further technological advancements in the continuous synthesis of sodium acrylate. The technological aspects of the process development for the synthesis of acrylic acids salts are outlined in a series of patents.[107–110]

It is worth noting that Chevron chemists also attempted to develop a technological process using nickel complexes. In their 2018 patent[111] they utilized a salt form of ion-exchange polystyrene resin with sulfonate, phosphonate, sulfinate, thiosulfonate and thiosulfinate groups as a base, including commercial resins such as Amberlite and Amberlyst. This modification simplifies the separation of the solid pure reaction product from the catalyst. However, the acrylate yield reported in the patent when using the sodium salt of Amberlite resin was only 6.7%. It is impossible to assess the effectiveness of using other resins based on the information provided in the patent.

In the next patent by these authors[112] the following modified metal oxides were developed: chemically modified solid oxide (CMSO) and metal treated chemically modified solid oxide (MT-CMSO), which also acted as a heterogeneous base. The patent presents data for several modified oxides, among which the best acrylate yields were shown by aluminum oxide treated with sodium *tert*-butylate, as well as Amberlyst 36 resin treated with sodium *tert*-butylate. In the presence of $Ni(COD)_2$/dcpe catalytic system in toluene (CO_2/C_2H_4, 1 : 1, 20 bar, 100 °C, 6 h) and modified aluminum oxide, yields of more than 1200% as per nickel were achieved (Table 6). It is difficult to assess how convenient this reaction methodology is with respect to the use of Bu^tONa solution or suspension, but its efficiency was significantly lower (maximum TON = 12.4).

In the 2023 patent[113] the techniques for using metal oxides (CMSO, MT-CMSO) and ion exchange resins were improved and a nickel-containing catalyst deposited on such a carrier was proposed. The deposition on the oxide was carried out from THF *in situ* using Ni-lactone derived from $Ni(COD)_2$/dcpe in

Table 6. Synthesis[a] of sodium acrylate using CMSO.[112]

Carrier treated with ButONa	[Ni], mmol	Sodium acrylate (%)
Al_2O_3	0.2	218
Al_2O_3	0.02	1236
Amberlyst 36	0.2	158
Amberlyst 36	0.02	250
Amberlyst 36	0.002	561

[a] Conditions: $Ni(COD)_2$ (1 equiv.), dcpe (1.1 equiv.), toluene, ethylene (10 bar), CO_2 (10 bar), 100° C, 6 h.

CO_2/C_2H_4. These systems can catalyze the synthesis of acrylate not only in the presence of solvent, but also without a solvent, i.e. in a gas-phase heterogeneous system to achieve TON values up to 148 at 120 °C. A regeneration procedure was also proposed for the Ni-catalyst when its activity decreases. The main disadvantage of the process is the necessity to isolate the acrylic acid salt by solvent washing.

Interesting results were presented in the work by Vavasori with co-authors,[114] who showed that traditionally inactive monodentate phosphines (PPh_3, PBu^t_3) in Ni(0)-catalysis, as well as chelate diphosphines with a small 'bite angle' (*e.g.*, dtbpm and dppm),[79] work effectively as simple Ni(II) and Pd(II) complexes ($[NiCl_2(PPh_3)_2]$, $[PdCl_2(PPh_3)_2]$) in the synthesis of sodium acrylate. Under the specified conditions (Na-phenolate/[M] = 500/1 mol/mol; C_2H_4 (25 bar); CO_2 (25 bar); THF (25 mL); 90 °C; 20 h), good TON values on Ni(II) and Pd(II) (0.038 mol) of 280 and 222, respectively, are achieved, which decrease with decreasing catalyst loading. Bidentate ligands (dmmp, dppe, dppp, dppb, Xantphos) were tested, revealing a linear increase in catalyst TON with increasing phosphine 'bite angle'. It is shown that the TON value significantly increases with temperature with the dppp ligand showing an increase from 33 (at 30 °C) to 290 (at 130 °C) for the complex $[NiCl_2(dppp)]$, while the TON for $[PdCl_2(dppp)]$ increased from 3 (at 30 °C) to 111 (at 130 °C). The TON dependence on the type of base cation (Na^+ or K^+) and its concentration is also presented in this work. Curious results were obtained from the solvent screening of $[NiCl_2(dppp)]$, where the most effective were polar aprotic solvents — acetone (TON = 273) and DMSO (TON = 290), which had not been previously used in the catalytic synthesis of acrylate. Relatively high TONs were also achieved in alcoholic solvents with the best results in 1- and 2-propanols (TON = 261 and 244, respectively). However, despite the demonstrated results, the authors did not present a proposed mechanism of the process to explain how the catalytic system functions through the cationic forms of metals (Ni(II) and Pd(II)).

In addition to palladium and nickel compounds, systems based on rhodium and ruthenium complexes are active in the catalytic carboxylation of ethylene. In 1993 Aresta and Quaranta[99] observed the precipitation of solid Rh-lactone as a result of slow carboxylation (1 bar CO_2, THF, 25 °C, 9 days) of the ethylene complex (bpy)Rh(I)Cl(C_2H_4). Confirmation of the lactone structure was made based of NMR and IR spectroscopy data. In 2022, Nakao and co-workers[98] performed the catalytic synthesis of acrylates using pincer complexes of Rh with aminoguanidine ligands (Scheme 25). Hydride Rh(III)-complex **4a**, ethylene Rh(I)-complex **4b**, maleimide Rh(I)-complex **4c**, and the pincer phosphine complex **4d** were tested, with the pincer phosphine complex **4d** used for comparison. Complexes **4b,c** are derivatives of complex **4a** and are obtained by treatment of the latter with Bu^tOK in benzene, followed by complexation with ethylene or *N*-methylmaleimide. One of the key stages of synthesis, the coupling of ethylene and CO_2 to form Rh-lactone (78%), was confirmed by its synthesis from **4a**. However, the efficiency of this system remains low with a maximum TON of 7.7 at 160 °C. The transition from low-polarity solvents such as toluene and anisole to dimethylacetamide does not result in increased efficiency.

Iwasawa and co-workers[97] obtained very interesting results on Ru(0) derivatives. First, the authors synthesized the known

Scheme 25

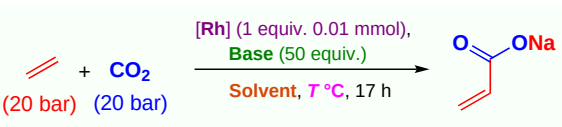

[Rh]	Solvent	T, °C	Base	TON
4a[a]	PhH	160	Bu^tONa	**16**
4b[a]	PhH	160	Bu^tONa	**15**
4c[a]	PhH	160	Bu^tONa	**16**
4d	PhH	160	Bu^tONa	**0.1**
4c	PhH	140	Bu^tONa	**2.3**
4c	PhH	160	Bu^tONa	**11**
4c	PhH	180	Bu^tONa	**2.5**
4c	PhMe	160	Bu^tONa	**7.7**
4c	PhOMe	160	Bu^tONa	**6.0**
4c	DMA	160	Bu^tONa	**4.0**
4c	THF	160	Bu^tONa	**11**
4c	PhH	160	ArONa[b]	**1.6**
4c[a]	DMA	160	Na_2CO_3	**0.2**
4c[a]	DMA	160	Cs_2CO_3	**4.2**

[a] 5.0 mmol [Rh], base 100 equiv.; [b] Ar = 2,6-diMePh

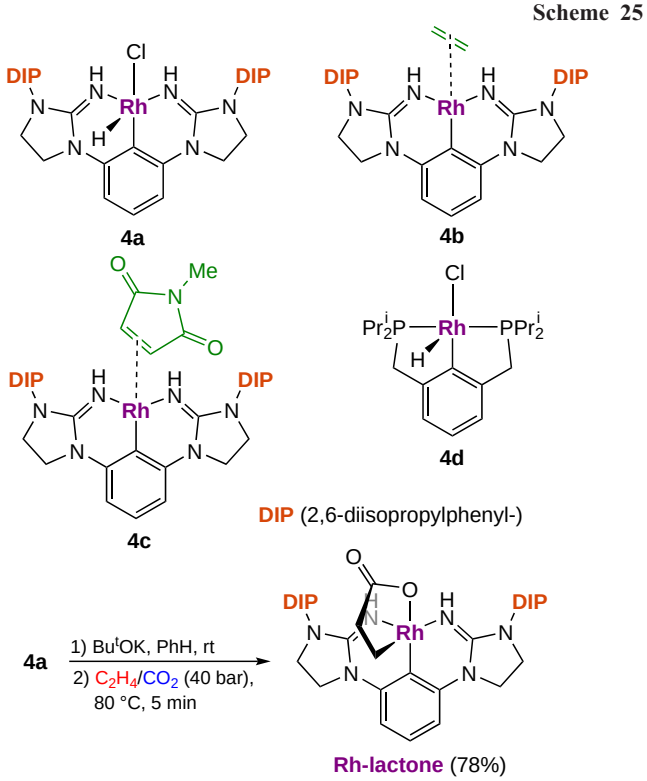

Scheme 26

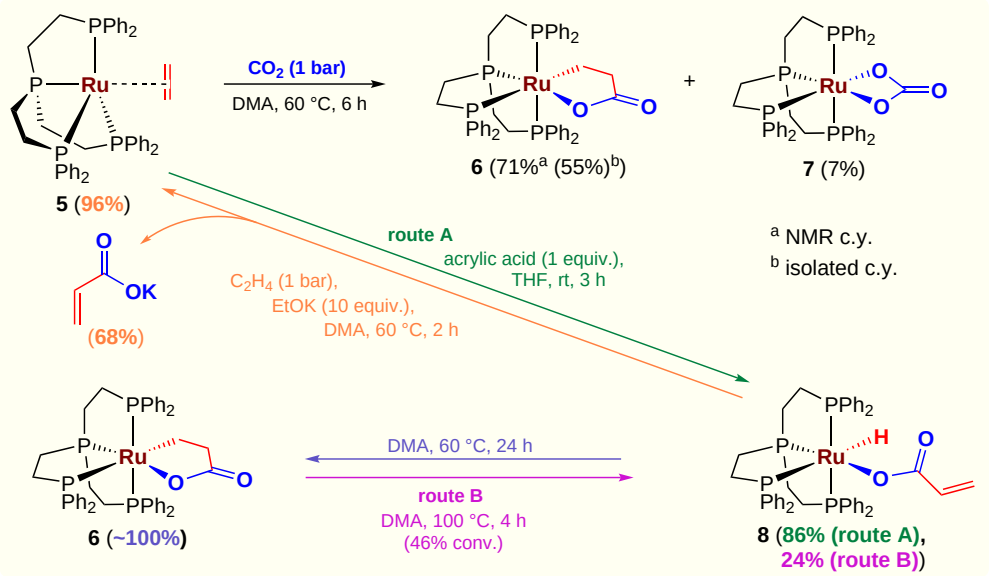

stabilized by tetradentate phosphine ligand ethylene complex of Ru(0) **5**,[115,116] and then investigated its ability to form Ru-lactone **6** (Scheme 26).

The yield of **6** in direct coupling of the ethylene complex **5** with CO_2 is 71% by NMR and 55% in the isolated form. In this process all transformations for ruthenium are of equilibrium character, allowing for a complete catalytic cycle from any intermediates. Particularly, the exchange of the acrylate fragment in **8** to ethylene (route A) in the presence of potassium ethylate proceeds with an efficiency of 96%. Meanwhile, the crucial key step of *β*-elimination in Ru-lactone (route B) to form a hydride complex of acrylate **8** (24%) proceeds simply upon heating to 100 °C. The reverse process of recyclization to lactone **6** proceeds at 60 °C in quantitative yield. Although the catalytic efficiency was rather low (maximum TON = 6) compared to nickel and palladium systems, this was the first example of catalytic synthesis of acrylate from ethylene and CO_2 using a ruthenium catalyst (Scheme 27).

Due to the ease of transforming Ru-lactone into acrylate through simple thermal rearrangement without the need for any additives, this system shows promise for further development. Therefore, Iwasawa with co-authors [117] continued their research to develop new more efficient catalysts. They synthesized a series of tetradentate phosphine ligands **L1**–**4** with varying donor abilities and framework rigidities (Scheme 28).

The preparation of Ru complexes based on **L1-4** ligands was carried out in two steps. First, the **Ru1-4-OAc** hydride-acetate

Scheme 27

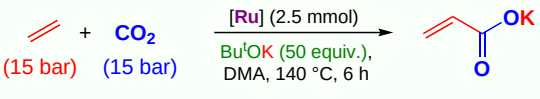

[Ru]	TON
1	**2**
1[a]	**6**
$RuCl_2(PPh_3)$	<1
$Ru_3(CO)_{12}$	<1
$Ru(CO)_2(PPh_3)_3$	<1

[a] [Ru] (10 mmol), ButOK (250 equiv.), 12 h

complexes were prepared in good yield, and then ethylene complexes of **Ru1-4** were synthesized by treatment with ButOK in an ethylene atmosphere. Based on the NMR chemical shifts of carbon atoms of coordinated ethylene **Ru1** (18.6 ppm) > **Ru2** (22.1 ppm) > **Ru3** (34.8 ppm) > **Ru4** (43.1 ppm), the donor ability of phosphine ligands was determined to be in the following order **L1** > **L2** > **L3** > **L4**. The more donor complexes of ethylene are more rapidly transformed into Ru-lactone (*e.g.*, **Ru3** for 15 h and **Ru1** for 1 h at 60 °C, whereas **Ru4** does not react at all) as well as into an acrylate complex (in CO_2/ethylene mixture) of type **4** (see Scheme 26) and then successively enter into rapid exchange with ethylene in the presence of ButOK, regenerating the initial **Ru1** complex.

As a result of studying the effect of different strengths of bases on the rate of transformation of Ru-lactone into the **Ru3** ethylene complex, it was concluded that there are two pathways for this process (Scheme 29).

According to the authors, in the case of a strong base, pathway 2 is realized with initial proton abstraction from the lactone. In the case of a weak base two pathways can be realized depending on the amount of base present. Testing of **Ru1-4-OAc** complexes in an actual catalytic process with ButOK revealed that the most active derivatives of ligands **L1** and **L2** only produced substoichiometric amounts of acrylate. However, the least active **Ru4-OAc** complex was catalytically active in the lactone formation process (TON = 7.9). Additionally, transitioning to the weaker bases CsOMes and Cs_2CO_3 slightly increased the yield of acrylate. In the latter case, the **Ru4** ethylene complex exhibited the highest TON = 15 with a 1000-fold excess of the weak base and a 4-fold increase in **Ru4** loading. Despite this excess, the use of stable cesium carbonate is very convenient for practical applications and demonstrates the characteristic pathway 1 for ruthenium.

At the current stage of research on Ru-catalytic systems, there is insufficient knowledge to understand the ways of catalyst deactivation and how to increase their catalytic efficiency. However, the unique properties of Ru-catalysts that allow for the conversion of the lactone ring into an acrylate fragment under moderate heating conditions make Ru-systems promising for future improvements. It is possible, that they will undergo the same rapid growth of interest and application as we have seen with Ru-catalysts in Grubbs metathesis, which are utilized on both laboratory and industrial scales.

Scheme 28

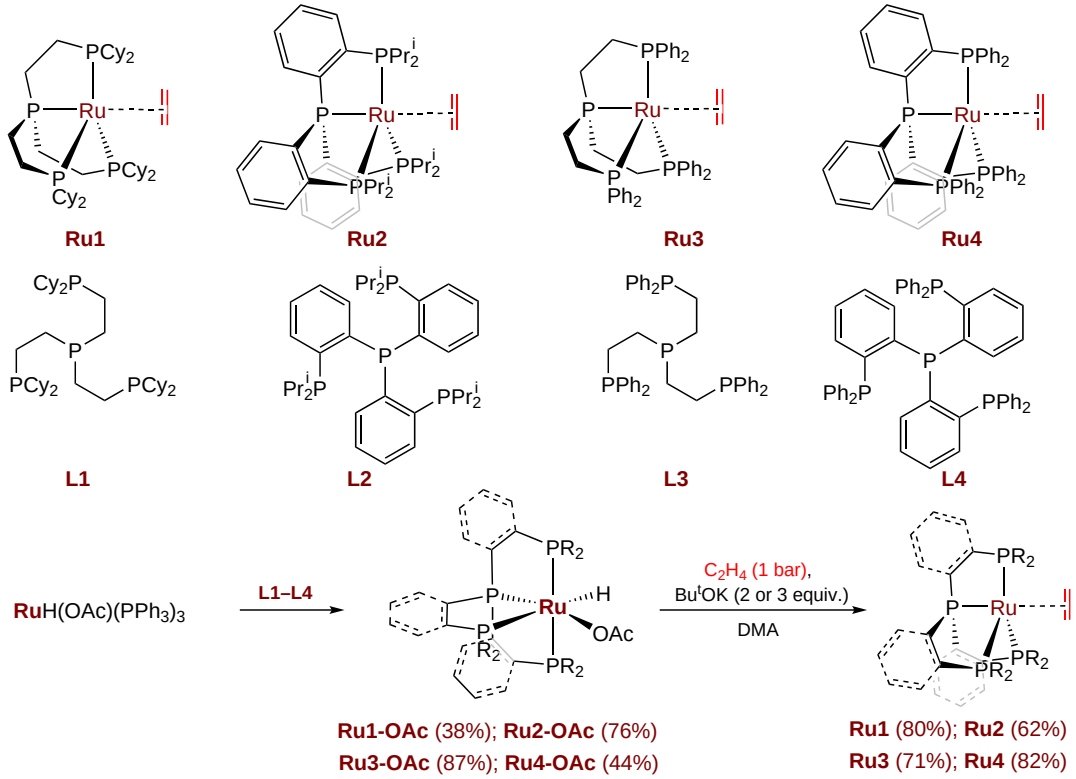

Scheme 29

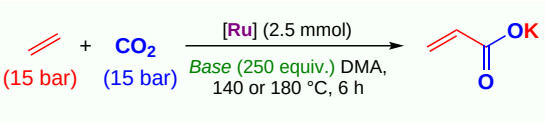

[Ru]	Base	TON	
		140 °C	180 °C
Ru1-OAc	ButOK	**0.3**	**0.3**
Ru2-OAc	ButOK	**0.2**	**0.4**
Ru3-OAc	ButOK	**1.5**	**1.1**
Ru4-OAc	ButOK	**0.7**	**7.9**
Ru4-OAc	K_2CO_3	–	**0.6**
Ru4-OAc	CsOMes	–	**8.8**
Ru4-OAc	Cs_2CO_3	–	**8.6**
Ru4[a]	Cs_2CO_3	–	**15**

[a] **[Ru]** (10 mmol), Cs_2CO_3 (1000 equiv.)

Proposed two pathways for the cleavage of Ru-lactone

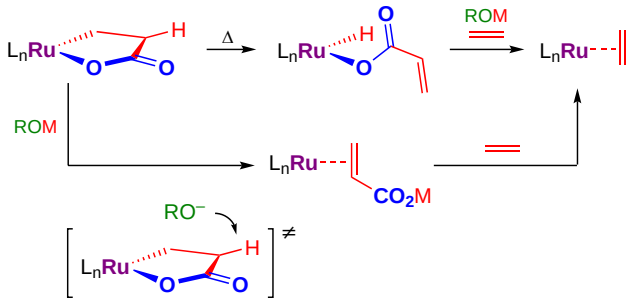

4. Conclusion

This review was written under the influence of the discovery that the reaction of ethylene with CO_2 to form the AA salt is quite attainable if suitable conditions (catalysts, additives, base or Lewis acid, solvent, temperature and pressure) are used. It is crucial to note that, unlike the synthesis of AA itself, synthesis of acrylate is exothermic and thermodynamically allowed. However, overcoming thermodynamics does not guarantee acceptable kinetics, as the TON values are still relatively low. The mechanism of this reaction, particularly the decay of the metallacycle and the *β*-elimination of hydrogen, is not fully understood, as it can involve both *β*-hydride and *β*-proton abstraction. The fact that the reaction can be catalyzed by LiI in the absence of a base and can also achieve high (according to available numbers) TOF values with strong bases like ButONa, complicates drawing a definitive conclusion. Nevertheless, it can be affirmed that the catalytic coupling of ethylene and CO_2 (direct carboxylation) to form sodium acrylate is a viable synthetic method, that has evolved from a theoretical concept, a ‘dream reaction’, to a technologically advanced process. Initial studies on Ni catalysts show promise but suffer from low stability, hindering catalyst recycling and industrial application. Utilization of more stable mixed nickel phosphine-carbene complexes could enhance the industrial potential of Ni systems. Additionally, simple and stable catalytic systems based on $[Pd(PPh_3)_4]$ have been identified. Optimization their conditions of use has led to maximum efficiency in sodium acrylate preparation (TON >500), catalyst recycling without loss of efficiency and full utilization of cost-effective bases like sodium isopropylate or sodium *tert*-butylate, derived directly from sodium hydroxide and alcohols. Analysis of scientific findings and patent data reveals industrial interest in this process, aiming to develop a competitive alternative to propylene oxidation for

AA production. However collaborative efforts are needed to realize this final step.

Acknowledgements

The article was prepared with the financial support of the Ministry of Science and Higher Education of the Russian Federation (agreement No. 075-15-2024-547 dated 24.04.2024).

5. List of abbreviations

AA — acrylic acid;
BARF — tetrakis[3,5-bis(trifluoromethyl)phenyl]borate;
BenzP* — 1,2-bis(*tert*-butylmethylphosphino)benzene;
CHP — *N*-cyclohexylpyrrolidone;
CMSO — chemically modified solid oxide;
COD — 1,5-cyclooctadiene;
DBF — *N*,*N*-dibutylformamide;
DBU — 1,8-diazabicyclo[5.4.0]undec-7-ene;
DCM — dichloromethane;
Dcpe — 1,2-bis(dicyclohexylphosphino)ethane;
Dcpp — 1,3-bis(dicyclohexylphosphino)propane;
DIPEA — diisopropyl ethylamine;
DFT — density functional theory;
DMA — *N*,*N*-dimethylacetamide;
Dmmp — dimethyl methyl phosphonate;
Dppe — 1,2-bis(diphenylphosphino)ethane;
Dppm — bis(diphenylphosphino)methane;
Dppp — 1,3-bis(diphenylphosphino)propane;
Dppb — 1,4-bis(diphenylphosphino)butane;
Dtbpe — 1,2-bis(di-*tert*-butylphosphino)ethane;
Dtbpm — bis(di-*tert*-butylphosphino)methane;
Dtbpp — 1,3-bis(di-*tert*-butylphosphino)propane;
DuanPhos — (1*R*)-2-*tert*-butyl-1-[(1*R*)-2-*tert*-butyl-1,3-dihydroisophosphinoindol-1-yl]-1,3-dihydroisophosphinindole;
IR — infrared;
Ir(dtbpy)$(ppy)_2$ PF_6 — 4,4′-bis(1,1-dimethylethyl)-2,2′-bipyridin-*N*1,*N*1′]bis[2-(2-pyridinyl-*N*)phenyl-*C*]iridium(III) hexafluorophosphate;
LED — light emission diode;
MT-CMSO — metal treated chemically modified solid oxide;
NHC — *N*-heterocyclic carbine;
NMP — *N*-Me-pyrrolidone;
Pr^{i}BenzP — 1,2-bis(di-*iso*-propylphosphino)benzene;
SAR — structure-activity relationship;
TangPhos — (1*S*,2*R*)-1-*tert*-butyl-2-[(1*S*,2*R*)-1-*tert*-butylphospholan-2-yl]phospholane;
TMEDA — *N*,*N*,*N*′,*N*′-tetramethylethylenediamine;
TOF — turnover frequency;
TON — turnover number;
UV — ultraviolet;
Xantphos — (9,9-dimethyl-9*H*-xanthene-4,5-diyl)bis(diphenylphosphane).

6. References

1. T.Ohara, T.Sato, N.Shimizu, G.Prescher, H.Schwind, O.Weiberg, K.Marten, H.Greim. In *Ullmann's Encyclopedia of Industrial Chemistry*. (Weinheim: Wiley-VCH, 2012)
2. M.Aresta, A.Dibenedetto, A.Angelini. *Chem. Rev*., **114**, 1709 (2014); https://doi.org/10.1021/cr4002758
3. X.-F.Wu, F.Zheng. *Top. Curr. Chem. (Z)*, **375**, 4 (2017); https://doi.org/10.1007/s41061-016-0091-6
4. A.Tortajada, F.Juliá-Hernández, M.Börjesson, T.Moragas, R.Martin. *Angew. Chem., Int. Ed*., **57**, 15948 (2018); https://doi.org/10.1002/anie.201803186
5. S.-S.Yan, Q.Fu, L.-L.Liao, G.-Q.Sun, J.-H.Ye, L.Gong, Y.-Z.Bo-Xue, D.-G.Yu. *Coord. Chem. Rev*., **374**, 439 (2018); https://doi.org/10.1016/j.ccr.2018.07.011
6. J.Artz, T.E.Muller, K.Thenert, J.Kleinekorte, R.Meys, A.Sternberg, A.Bardow, W.Leitner. *Chem. Rev*., **118**, 434 (2018); https://doi.org/10.1021/acs.chemrev.7b00435
7. S.Saini, P.K.Prajapati, S.L.Jain. *Catal. Rev.*, **64**, 631 (2020); https://doi.org/10.1080/01614940.2020.1831757
8. N.Yu.Kuznetsov, A.L.Maximov, I.P.Beletskaya. *Russ. J. Org. Chem*., **58**, 1681 (2022); https://doi.org/10.1134/S1070428022120016
9. N.N.Ezhova, N.V.Kolesnichenko, A.L.Maximov. *Pet. Chem.*, **62**, 40 (2022); https://doi.org/10.1134/S0965544122010078
10. R.Chatterjee, A.Bhaumik. *Curr. Org. Chem*., **26**, 60 (2022); https://doi.org/10.2174/1385272825666211206090621
11. C.-K.Ran, H.-Z.Xiao, L.-L.Liao, T.Ju, W.Zhang, D.-G.Yu. *Natl. Sci. Open*, **2**, 20220024 (2023); https://doi.org/10.1360/nso/20220024
12. J.-H.Ye, T.Ju, H.Huang, L.-L.Liao, D.-G.Yu. *Chem. Res.*, **54**, 2518 (2021); https://doi.org/10.1021/acs.accounts.1c00135
13. M.Borjesson, T.Moragas, D.Gallego, R.Martin. *ACS Catal*., **6**, 6739 (2016); https://doi.org/10.1021/acscatal.6b02124
14. S.Dabrala, T.Schauba. *Adv. Synth. Catal*., **361**, 223 (2019); https://doi.org/10.1002/adsc.201801215
15. Y.Yang, J.-W.Lee. *Chem. Sci*., **10**, 3905 (2019); https://doi.org/10.1039/c8sc05539d
16. D.N.Gorbunov, M.V.Nenasheva, M.V.Terenina, Yu.S.Kardasheva, S.V.Kardashev, E.R.Naranov, A.L.Bugaev, A.V.Soldatov, A.L.Maximov, E.A.Karakhanov. *Pet. Chem.*, **62**, 1 (2022); https://doi.org/10.1134/S0965544122010054
17. A.L.Maximov, I.P.Beletskaya. *Russ. Chem. Rev.*, **93** (1), RCR5101 (2024); https://doi.org/10.59761/RCR5101
18. M.Melieres, C.Marechal. *Climate Change: Past, Present and Future*. (1st Edn). (UK: Wiley, 2015). P. 285
19. M.Oppenheimer, B.C.Glavovic, J.Hinkel, R.van de Wal, A.K.Magnan, A.Abd-Elgawad, R.Cai, M.Cifuentes-Jara, R.M.DeConto, T.Ghosh, J.Hay, F.Isla, B.Marzeion, B.Meyssignac, Z.Sebesvari. *IPCC Special Report on the Ocean and Cryosphere in a Changing Climate*. (Eds H.-O.Portner, D.C.Roberts, V.Masson-Delmotte, P.Zhai, M.Tignor, E.Poloczanska, K.Mintenbeck, A.Alegría, M.Nicolai, A.Okem, J.Petzold, B.Rama, N.M.Weyer). (Cambridge: Cambridge University Press, 2019). P. 321; https://doi.org/10.1017/9781009157964.006
20. J.Hjort, D.Streletskiy, G.Doré, Q.Wu, K.Bjella, M.Luoto. *Nat. Rev. Earth Environ*., **3**, 24 (2022); https://doi.org/10.1038/s43017-021-00247-8
21. R.Tanaka, M.Yamashita, K.Nozaki. *J. Am. Chem. Soc*., **131**, 14168 (2009); https://doi.org/10.1021/ja903574e
22. B.G.Schieweck, N.F.Westhues, J.Klankermayer. *Chem. Sci*., **10**, 6519 (2019); https://doi.org/10.1039/C8SC05230A
23. M.Limbach. *Adv. Organomet. Chem*., **63**, 175 (2015); https://doi.org/10.1016/bs.adomc.2015.03.001
24. M.Hollering, B.Dutta, F.E.Kühn. *Coord. Chem. Rev*., **309**, 51 (2016); https://doi.org/10.1016/j.ccr.2015.10.002
25. X.Wang, H.Wang, Y.Sun. *Chem*, **3**, 211 (2017); https://doi.org/10.1016/j.chempr.2017.07.006
26. T.Schaub. In *Organometallics in Process Chemistry. Topics in Organometallic Chemistry*. Vol. 65. **(**Eds T.Colacot, V.Sivakumar). (Cham: Springer, 2018); https://doi.org/10.1007/3418_2018_21
27. T.Schaub, A.S.K.Hashmi, R.A.Paciello. *J. Org. Chem*., **84**, 4604 (2019); https://doi.org/10.1021/acs.joc.8b02362
28. K.Zimmerschied. *Congr. FATIPEC*, **19**, 105 (1988)

29. R.Cox. In *Synthetic Fibres: Nylon, Polyester, Acrylic, Polyolefin*. Ch. 4. (Ed. J.E.McIntyre). (Woodhead Publishing, 2004)
30. EP123 482-B (1986)
31. Patent US 4541935 (1985)
32. Patent US 4673402 (1987)
33. Patent US 4364992 (1982)
34. Patent US 4675012 (1987)
35. Patent US 4519799 (1985)
36. M.Frank. In *Ullmann's Encyclopedia of Industrial Chemistry*. (Weinheim: Wiley-VCH, 2012)
37. Patent JP 88 046724-B (1988)
38. Patent US 3330729 (1967)
39. Patent EP 77 618-B (1986)
40. W.Reppe. *Modern Plastics*, **23**, 162 (1945); [*Chem. Abs*., **40**, 1449 (1946)]
41. S.Li. *Manufacture of Fine Chemicals from Acetylene*. (Berlin, Boston: De Gruyter, 2021); https://doi.org/10.1515/9783110714999
42. Patent US 3023237A (1962)
43. Patent WO 2017/165344A1 (2017)
44. Patent US 2020/0325093A1 (2020)
45. H.A.Witcoff, B.G.Reuben, J.S.Plotkin. *Industrial Organic Chemicals*. (3rd Ed.). (Hoboken: Wiley & Sons, 2013)
46. *Encyclopedia of Chemical Technology*. Vol. 1. (Ed. J.I.Kroschwitz). (John Wiley & Sons, 1991). P. 357
47. J.L.Rodrigues. *SynBio*, **1**, 3 (2023); https://doi.org/10.3390/synbio1010002
48. U.C.Abubakar, Y.Bansod, L.Forster, V.Spallina, C.D'Agostino. *React. Chem. Eng*., **8**, 1819 (2023); https://doi.org/10.1039/D3RE00057E
49. M.M.Buitelaar, E.van Daatselaar, D.G.van Teijlingen, H.I.Stokvis, J.D.Wendt, R.J.De Sousa Ribeiro, A.M.M.Brooks, E.C.Kamphuis, S.Lopez Montoya, J.C.van Putten, A.G.J.van der Ham, H.van den Berg, J.-P.Lange. *Ind. Eng. Chem. Res*., **59**, 1183 (2020); https://doi.org/10.1021/acs.iecr.9b04334
50. H.Lin, W.M.Hui, K.Sibudjing. *React. Chem. Eng*., **8**, 502 (2023); https://doi.org/10.1039/D2RE00462C
51. J.G.H.Hermens, A.Jensma, B.L.Feringa. *Angew. Chem., Int. Ed*., **61**, e202112618 (2022); https://doi.org/10.1002/anie.202112618
52. A.Massó Ramírez, F.Ivars-Barceló, J.M.López Nieto. *Catal. Today*, **356**, 322 (2020); https://doi.org/10.1016/j.cattod.2019.10.030
53. Patent US 6043184 (2000)
54. Patent US 6500982 (2002)
55. Patent FR 2855514 (2003)
56. Patent US 7019169 (2004)
57. P.J.Chenier. In *Topics in Applied Chemistry*. (3rd Ed.). (Springer Science & Business Media, 2002)
58. M.Aresta, C.F.Nobile, V.G.Albano, E.Forni, M.Manassero. *J. Chem. Soc., Chem. Commun*., 636 (1975); https://doi.org/10.1039/C39750000636
59. M.Aresta, R.Gobetto, E.Quaranta, I.Tommasi. *Inorg. Chem*., **31**, 4286 (1992); https://doi.org/10.1021/ic00047a015
60. M.Aresta, A.Dibenedetto, E.Quaranta. In *Carbon Dioxide Conversion*. (Berlin, Heidelberg: Springer-Verlag, 2016)
61. S.Bierbaumer, M.Nattermann, L.Schulz, R.Zschoche, T.J.Erb, C.K.Winkler, M.Tinzl, S.M.Glueck. *Chem. Rev.*, **123**, 5702 (2023); https://doi.org/10.1021/acs.chemrev.2c00581
62. H.Hoberg, D.Schaefer. *J. Organomet. Chem*., **236**, C28 (1982); https://doi.org/10.1016/S0022-328X(00)86765-0
63. H.Hoberg, D.Schaefer, G.Burkhart, C.Kruger, M.Romao. *J. Organomet. Chem*., **266**, 203 (1984); https://doi.org/10.1016/0022-328X(84)80129-1
64. H.Hoberg, B.W.Oster. *J. Organomet. Chem*., **266**, 321 (1984); https://doi.org/10.1016/0022-328X(84)80145-X
65. H.Hoberg, D.Schaefer. *J. Organomet. Chem*., **251**, C51 (1983); https://doi.org/10.1016/S0022-328X(00)98789-8
66. D.Walther, E.Dinjus. *Z. Chem.*, **22**, 228 (1982); https://doi.org/10.1002/zfch.19840240815
67. D.Walther, E.Dinjus, J.Sieler, N.N.Thanh, W.Schade, I.Leban. *Z. Naturforsch. B*, **38**, 835 (1983); https://doi.org/10.1515/znb-1983-0709
68. H.Hoberg, Y.Peres, A.Milchereit. *J. Organomet. Chem*., **307**, C38 (1986); https://doi.org/10.1016/0022-328X(86)80487-9
69. H.Hoberg, Y.Peres, C.Krüger, Y.H.Tsay. *Angew. Chem., Int. Ed*., **26**, 771 (1987); https://doi.org/10.1002/anie.198707711
70. R.Fischer, J.Langer, H.Gorls, A.Malassa, D.Walther, G.Vaughan. *Chem. Commun*., **23**, 2510 (2006); https://doi.org/10.1039/B603540J
71. C.Bruckmeier, M.W.Lehenmeier, R.Reichardt, S.Vagin, B.Rieger. *Organometallics*, **29**, 2199 (2010); https://doi.org/10.1021/om100060y
72. S.Y.T.Lee, M.Cokoja, M.Drees, Y.Li, J.Mink, W.A.Herrmann, F.E.Kuhn. *ChemSusChem*, **4**, 1275 (2011); https://doi.org/10.1002/cssc.201000445
73. P.N.Plessow, L.Weigel, R.Lindner, A.Schafer, F.Rominger, M.Limbach, P.Hofmann. *Organometallics*, **32**, 3327 (2013); https://doi.org/10.1021/om400262b
74. Y.Zhu, X.Guo, X.Ding, L.Sun, M.Zhang, Z.Liu. *Mol. Catal.*, **518**, 112108 (2022); https://doi.org/10.1016/j.mcat.2021.112108
75. M.L.Lejkowski, R.Lindner, T.Kageyama, G.É.Bódizs, P.N.Plessow, I.B.Müller, A.Schäfer, F.Rominger, P.Hofmann, C.Futter, S.A.Schunk, M.Limbach. *Chem. – Eur. J.*, **18**, 14017 (2012); https://doi.org/10.1002/chem.201201757
76. D.C.Graham, C.Mitchell, M.I.Bruce, G.F.Metha, J.H.Bowie, M.A.Buntine. *Organometallics*, **26**, 6784 (2007); https://doi.org/10.1021/om700592w
77. D.Jin, P.G.Williard, N.Hazari, W.H.Bernskoetter. *Chem. – Eur. J.*, **20**, 3205 (2014); https://doi.org/10.1002/chem.201304196
78. C.Hendriksen, E.A.Pidko, G.Yang, B.Schaffner, D.Vogt. *Chem. – Eur. J.*, **20**, 12037 (2014); https://doi.org/10.1002/chem.201404082
79. N.Huguet, I.Jevtovikj, A.Gordillo, M.L.Lejkowski, R.Lindner, M.Bru, A.Y.Khalimon, F.Rominger, S.A.Schunk, P.Hofmann, M.Limbach. *Chem. – Eur. J*., **20**, 16858 (2014); https://doi.org/10.1002/chem.201405528
80. M.N.Hopkins, K.Shimmei, K.B.Uttley, W.H.Bernskoetter. *Organometallics*, **37**, 3573 (2018); https://doi.org/10.1021/acs.organomet.8b00260
81. K.B.Uttley, K.Shimmei, W.H.Bernskoetter. *Organometallics*, **39**, 1573 (2020); https://doi.org/10.1021/acs.organomet.9b00708
82. S.Manzini, N.Huguet, O.Trapp, R.A.Paciello, T.Schaub. *Catal. Today*, **281**, 379 (2017); https://doi.org/10.1016/j.cattod.2016.03.025
83. K.Takahashi, K.Cho, A.Iwai, T.Ito, N.Iwasawa. *Chem. – Eur. J.*, **25**, 13504 (2019); https://doi.org/10.1002/chem.201903625
84. J.Kim, H.Hahm, J.Y.Ryu, S.Byun, D.-A.Park, S.H.Lee, H.Lim, J.Lee, S.Hong. *Catalysts*, **10**, 758 (2020); https://doi.org/10.3390/catal10070758
85. K.Takahashi, Y.Sakurazawa, A.Iwai, N.Iwasawa. *ACS Catal*., **12**, 3776 (2022); https://doi.org/10.1021/acscatal.2c01053
86. H.Hoberg, A.Ballesteros, A.Sigan, C.Jégat, D.Bärhausen, A.Milchereit. *J. Organomet. Chem*., **407**, C23 (1991); https://doi.org/10.1016/0022-328X(91)86320-P
87. R.Ayyappan, I.Abdalghani, R.C.Da Costa, G.R.Owen. *Dalton Trans*., **51**, 11582 (2022); https://doi.org/10.1039/D2DT01609E
88. S.A.Cohen, J.E.Bercaw. *Organometallics*, **4**, 1006 (1985); https://doi.org/10.1021/om00125a008
89. H.G.Alt, C.E.Denner. *J. Organomet. Chem*., **390**, 53 (1990); https://doi.org/10.1016/0022-328X(90)80156-T
90. B.Hessen, A.Meetsma, F.Van Bolhuis, J.H.Teuben, G.Helgesson, S.Jagner. *Organometallics*, **9**, 1925 (1990); https://doi.org/10.1021/om00156a037

91. R.Alvarez, E.Carmona, A.Galindo, E.Gutierrez, J.M.Marin, A.Monge, M.L.Poveda, C.Ruiz, J.M.Savariault. *Organometallics*, **8**, 2430 (1989); https://doi.org/10.1021/om00112a026
92. R.Alvarez, E.Carmona, D.J.Cole-Hamilton, A.Galindo, E.Gutierrez-Puebla, A.Monge, M.L.Poveda, C.Ruiz. *J. Am. Chem. Soc*., **107**, 5529 (1985); https://doi.org/10.1021/ja00305a037
93. M.Alvarez, A.Galindo, P.J.Perez, E.Carmona. *Chem. Sci*., **10**, 8541 (2019); https://doi.org/10.1039/C9SC03225H
94. T.T.Adamson, S.P.Kelley, W.H.Bernskoetter. *Organometallics*, **39**, 3562 (2020); https://doi.org/10.1021/acs.organomet.0c00528
95. S.M.Rummelt, H.Zhong, I.Korobkov, P.J.Chirik. *J. Am. Chem. Soc*., **140**, 11589 (2018); https://doi.org/10.1021/jacs.8b07558
96. H.Hoberg, K.Jenni, K.Angermund, C.Krueger. *Angew. Chem., Int. Ed.*, **26**, 153 (1987); https://doi.org/10.1002/anie.198701531
97. T.Ito, K.Takahashi, N.Iwasawa. *Organometallics*, **38**, 205 (2019); https://doi.org/10.1021/acs.organomet.8b00789
98. S.Takegasa, M.M.Lee, K.Tokuhiro, R.Nakano, M.Yamashita. *Chem. – Eur. J*., **28**, e202201870 (2022); https://doi.org/10.1002/chem.202201870
99. M.Aresta, E.Quaranta. *J. Organomet. Chem*., **463**, 215 (1993); https://doi.org/10.1016/0022-328X(93)83420-Z
100. S.C.E.Stieber, N.Huguet, T.Kageyama, I.Jevtovikj, P.Ariyananda, A.Gordillo, S.A.Schunk, F.Rominger, P.Hofmann, M.Limbach. *Chem. Commun*., **51**, 10907 (2015); https://doi.org/10.1039/C5CC01932J
101. I.Knopf, M.-A.Courtemanche, C.C.Cummins. *Organometallics*, **36**, 4834 (2017); https://doi.org/10.1021/acs.organomet.7b00734
102. A.O'Reilly, M.G.Gardiner, C.L.McMullin, J.R.Fulton, M.P.Coles. *Chem. Commun*., **60**, 881 (2024)
103. Y.Sasaki, Y.Inoue, H.Hashimoto. *J. Chem. Soc., Chem. Commun*., 605 (1976); https://doi.org/10.1039/C39760000605
104. A.Musco, C.Perego, V.Tartiari. *Inorg. Chim. Acta*, **28**, L147 (1978); https://doi.org/10.1016/S0020-1693(00)87385-5
105. S.Manzini, N.Huguet, O.Trapp, T.Schaub. *Eur. J. Org. Chem*., 7122 (2015); https://doi.org/10.1002/ejoc.201501113
106. S.Manzini, A.Cadu, A.-C.Schmidt, N.Huguet, O.Trapp, R.Paciello, T.Schaub. *ChemCatChem*, **9**, 2269 (2017); https://doi.org/10.1002/cctc.201601150
107. Patent WO 2015173276 (2015)
108. Patent WO 2015173277 (2015)
109. Patent WO 2016180775 (2016)
110. Patent WO 2017178282 (2017)
111. Patent US 2018/0362434 Al (2018)
112. Patent US 2018/0362434 Al (2020)
113. Patent US 2023/0192586 Al (2023)
114. A.Vavasori, L.Calgaro, L.Pietrobon, L.Ronchin. *Pure Appl. Chem*., **90**, 315 (2018); https://doi.org/10.1515/pac-2017-0706
115. C.Bianchini, P.J.Perez, M.Peruzzini, F.Zanobini, A.Vacca. *Inorg. Chem*., **30**, 279 (1991); https://doi.org/10.1021/ic00002a024
116. R.Osman, D.I.Pattison, R.N.Perutz, C.Bianchini, J.A.Casares, M.Peruzzini. *J. Am. Chem. Soc*., **119**, 8459 (1997); https://doi.org/10.1021/ja963797w
117. K.Takahashi, Y.Hirataka, T.Ito, N.Iwasawa. *Organometallics*, **39**, 1561 (2020); https://doi.org/10.1021/acs.organomet.9b00659